ŠIAULIŲ UNIVERSITETAS
INŽINERIJOS KATEDRA

Sourabh, Sukumar Ketkale

JŪROS DUMBLIŲ AUGINIMO MODULIO STIPRUMO TYRIMAS

Magistro darbas

ŠIAULIAI, 2018

ŠIAULIŲ UNIVERSITETAS
INŽINERIJOS KATEDRA

TVIRTINU
Katedros vedėja

Ramunė Klevaitytė

2018-05-31

JŪROS DUMBLIŲ AUGINIMO MODULIO STIPRUMO TYRIMAS

Magistro darbas

Vadovas

Doc. dr. Sergėjus Rimovskis
2018-05-31

Recenzentas

Doc. dr. Artūras Sabaliauskas
2018-05-31

Atliko

MM-16 gr. stud.
Sourabh, Sukumar Ketkale
2018-05-31

ŠIAULIAI, 2018

ŠIAULIŲ UNIVERSITY
ENGINEERING DEPARTMENT

Sourabh, Sukumar Ketkale

STRENGTH ANALYSIS OF SEAWEED CULTIVATION MODULE

Master Thesis

ŠIAULIAI, 2018

ŠIAULIŲ UNIVERSITETAS
ENGINEERING DEPARTMENT

APPROVED

Head of Department

2018-05-31

STRENGTH ANALYSIS OF SEAWEED CULTIVATION MODULE

Master Thesis

Guide

Doc. dr. Sergėjus Rimovskis
2018-05-31

Evaluator

Doc. dr. Artūras Sabaliauskas
2018-05-31

Conducted

stud. of MM-16 gr.
Sourabh, Sukumar Ketkale
2018-05-31

ŠIAULIAI, 2018

ACKNOWLEDGEMENT

I take this opportunity to thank Šiauliai University for the support.

I take this opportunity to thank Doc. Dr. Sergėjus Rimovskis (Guide) for providing continuous support throughout the project.

I am also grateful to Jonas Kamašauskas and Metal Production, for guiding and providing the details for project.

I also take this opportunity to thank my parents and friends for their moral support and believing in me.

TVIRTINU
Mechanikos ir statybos inžinerijos katedros vedėja
__________ Loreta Kelpšienė
2017 m. vasario mėn. 6 d.

MAGISTRO DARBO UŽDUOTIS

Išduota magistrantui: Sourabh, Sukumar Ketkale

Darbo tema: Strenght analysis of seaweed cultivation module

Galutinai patvirtinta 2018 m. kovo 7 d. katedros posėdžio protokolu Nr. INZK-3-3.

1. Darbo tikslas

To analyze the structure of seaweed module and to simulate its strength for different loads (immersion depth, sea stream).

2. Darbo struktūra

1. Introduction.
2. Analysis of the seaweed cultivation module structure and conditions of usage.
3. Simulation of the seaweed cultivation module strenght with Solidworks Simulation.
4. Analysis of results.
5. Conclusions.
6. References.

Darbo pateikimo terminas 2018 m. birželio mėn. 1 d.

Užduotį gavau Sourabh, Sukumar Ketkale (magistranto vardas, pavardė) __________ (parašas, data) 2017-02-06

Vadovas Sergėjus Rimovskis (pareigos, vardas, pavardė) __________ (parašas, data) 2017-02-06

TABLE OF CONTENTS

ŠIAULIŲ UNIVERSITETAS

INŽINERIJOS KATEDRA

SOURABH SUKUMAR KETKALE. JŪROS DUMBLIŲ AUGINIMO MODULIO STIPRUMO TYRIMAS vadovas doc. dr. S. Rimovskis

SANTRAUKA

Šiame magistro darbe nagrinėjamas jūros dumblių auginimo modulis, kuris buvo suprojektuotas Lietuvos įmonės UAB Metal Production konstruktorių. Padedant įmonės darbuotojams ir Šiaulių universiteto dėstytojams, buvo išstudijuota modulio konstrukcija, išsiaiškinta medžiagos (PE80) elgsena, esant užduotoms eksploatavimo sąlygoms. Buvo lyginami konstrukcijos įtempiai ir poslinkiai, esant skirtingoms apkrovoms, naudojant baigtinių elementų analizės sistemą Solidworks Simulation. Buvo pasirinkti skirtingi modulio panardinimo gyliai (iki 30 m), taip pat įvertintas ir jūros srovės poveikis. Buvo nustatyta, kad modulis yra suprojektuotas su tinkama atsarga.

Reikšminiai žodžiai: Jūros dumblių auginimo modulis, BEM, PE80 stiprumas

ŠIAULIAI UNIVERSITY
ENGINEERING DEPARTAMENT

SOURABH SUKUMAR KETKALE. STRENGTH ANALYSIS OF SEAWEED CULTIVATION MODULE supervisor assoc. prof. dr. S. Rimovskis.

SUMMARY

This master thesis is an attempt to a new approach in seaweed cultivation module that is attempted by an industry UAB Metal Production, Lithuania. With the support from Metal Production and Siauliai University it was tried to study and understand how the module made of PE80 will work under given conditions. The aim was to study the design of seaweed cultivation module, compare its stresses and displacements at different loading type with finite element modeling system Solidworks Simulation. Different depth of immersion (up to 30 m) is considered, as well as influence of see flow. It was determined that the module is designed within the factor of safety limits.

Keywords: Seaweed cultivation module, FEM, PE80 strength

List of Tables

List of Figures

THEME AND GOALS OF THE MASTER THESIS

THEME:

To analyze the design of seaweed module strength and check its behavior for different loads. To figure out the way hydrostatic pressure acts on the module.

GOALS:

- To analyze and apply fixtures at locations to constrain the body.
- To perform simulations for various depths with the basic data.
- To perform simulations for half structure and whole structure.
- To estimate the output available.
- To tabulate and compare the results.

1. INTRODUCTION

Seaweed is widely cultivated and eaten in Asia, sugar kelp (*Saccharina latissima*) is nutritious food that is rich in fibre, vitamins and minerals. It is used in food items like *sushi, soups, salads* and many other products. It is a cold water or winter crop.

Sugar kelp is marine algae, also known as sea belt and Devil's apron due to its shape. It is yellowish brown in color and looks like a giant lasagna noodle. It can grow up to 12 feet long. When dried, a white sweet-tasting powder forms on the frond. Long known as a sweetener and as a thickening and gelling agent that can be added to food and cosmetics, sugar kelp is being grown and harvested by more commercial firms in New England for a variety of uses, from food to potential biofuels. [1]

The spores grew into small plants less than one-tenth of an inch in size along string wound around a piece of PVC pipe. The spools with seeded lines were then transferred to aquaria for nursery culture in ultra-filtered seawater, where they grew well and quickly. At that point, the plants were ready to be placed in Long Island Sound to grow at Green Wave's ocean farm. The seeded line, unwound from the cylinder, was attached to a long rope, one of many growing lines on commercial underwater farms. Growing season ran from the late fall through the winter, before the water got too warm.

Fig. 1.1 Seaweed Kelp

2. MATERIAL

For many applications, the choice of material used depends upon a balance of stiffness, toughness, processability and price. For a particular application, a compromise between these features will usually be necessary. For example, it is generally true that, within a given family of grades of a particular polymer, the rigidity increases as impact strength decreases. Again, processing requirements may place an upper or a lower limit on the molecular weight (MW) of the polymer that can be used, and this will frequently influence the mechanical properties quite markedly. Single test values of a given property are a less reliable guide to operational behavior with plastics than with metals. This is because for plastics the great mass of empirical experience and tradition of effective design which has been built up over centuries in the field of metals is not yet available. Furthermore, no single value can be placed on the stiffness or the toughness of a plastic because:

- Stiffness will vary with time, stress and temperature.
- Toughness is influenced by the design and size of the component, the design of the mold, processing conditions and the temperature of use.
- Stiffness and toughness can be affected by environmental effects such as thermal and oxidative ageing, ultraviolet (UV) ageing and chemical attack (including the special case of environmental stress corrosion).

In addition, a change in a specific polymer parameter may affect processability and basic physical properties. Both of these factors can interact in governing the behavior of a fabricated article. Comprehensive experimental data are therefore necessary to understand effectively the behavior of plastic materials, and to give a realistic and reliable guide to the selection of material and grade.

In many applications, plastics are replacing traditional materials. Hence, there is often a natural tendency to apply to plastics tests similar to those that have been found suitable for gauging the performance of the traditional material. Dangers can obviously arise if plastics are selected on the basis of these tests without clearly recognizing that the correlation between values of laboratory performance and field performance may be quite different for the two classes of materials.

It is therefore important to realize that standard tests are not devised to give direct prediction of end-use performance. In general, the reverse is the case. That is, if a particular grade of a particular polymer is found to perform satisfactorily in a given end use, it can then be characterized with reasonable accuracy by standard tests, and the latter tests then used to ensure the maintenance of the required end-use quality. [2].

For seaweed cultivation module polyethylene pressure pipe, PE80- SDR11 is considered. Polyethylene has the simplest molecular structure of all polymers. It consists of two carbon and four hydrogen atoms in the basic repeating unit. Polyethylene is polymerized from ethylene gas that is obtained from natural gas or crude oil. The polymerization conditions of low temperature, low pressure, appropriate catalysts (such as Ziegler-Natta catalyst), and co-monomers result in a linear polyethylene. Linearity indicates that there are limited branches in the polymer chains, so that the molecules can pack tightly. High density polyethylene (HDPE) is one type of linear polyethylene with a density range from 0.941 to 0.965 g/cc as per ASTM D883. HDPE exhibits high strength and modulus; thus, it is preferred for use in the manufacture of plastic pipes [3].

Mechanical properties of the pipe considered for analysis are represented in the table 1.1 [4].

Table 1.1 Mechanical properties of PE80

	Property	Standard	Unit	**PE80**
	Density at 23°C	ISO 1183	g/cm^3	0,94
	Melt flow index	ISO 1133	g/10min	
	MFR 190/5			0,9
	MFR 190/2,16			
	MFR 230/5			
	MFI range	ISO1872/1873		T012
Mechanical Properties	Tensile stress at yield	ISO 527	MPa	20
	Elongation at yield	ISO 527	%	10
	Elongation at break	ISO 527	%	>600
	Impact strength unnotched at +23°C	ISO 179	kJ/m^2	no break
	Impact strength unnotched at -30°C			no break
	Impact strength notched at +23°C			12
	Impact strength notched at 0°C	ISO 179	kJ/m^2	
	Impact strength notched at -30°C			4,5
	Ball indentation hardness acc. Rockwell	ISO 2039-1	MPa	36
	Flexural strength (3,5% flexural stress)	ISO 178	MPa	18
	Modulus of elasticity	ISO 527	MPa	750

Stress vs. time

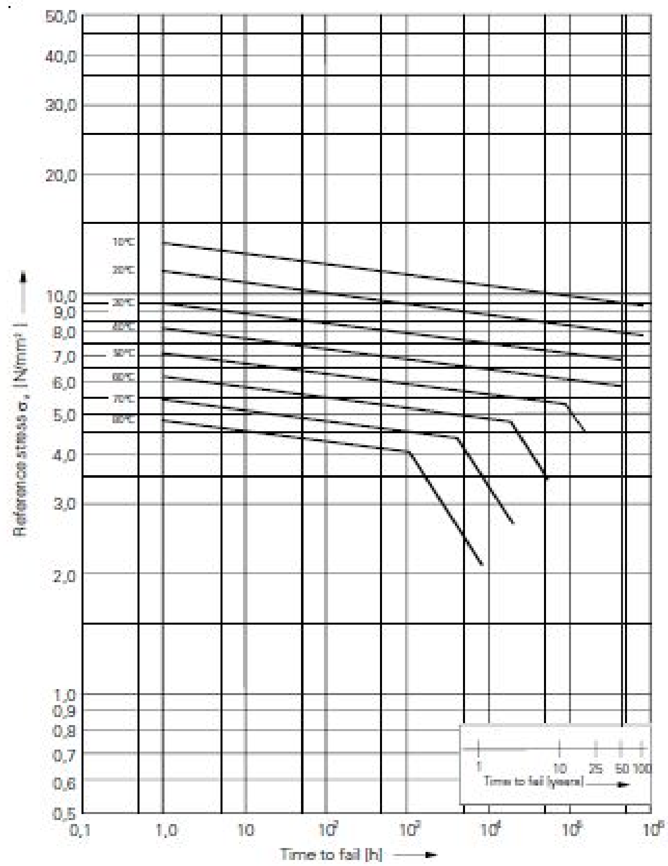

Fig. 2.1 Stress vs. Time graph of PE80

In Fig. 2.1 it is seen that how PE80 strength reduces over a period of 50 years at different temperatures. For current application sea water temperature considered is 20° C and the stress is reduced from 10- 11 MPa to 8 MPa over a period of 50 years, but these figures may change depending upon structure and fluid temperature [5].

Advantages of the material are listed as below [6]:

- Light weight of the pipes.
- Easy to fuse (weld).
- High abrasion resistance.
- Resistance to UV radiation.
- Resistance to radioactive effluent.
- Nontoxic.

- Elasticity. This property facilitates installation works.
- High tolerance of impact, as well as resistance to damage in bends.
- An important advantage choosing diameter of the pipes is low roughness due to the smooth internal walls of the pipes.
- Pipes are suitable for underwater installation, not influenced by sea water and its movement.
- Resistant (inert) to influence of the chemical substances.

3. HYDROSTATIC PRESSURE

The module is going to be placed underwater at different depths. Pressure in fluid at rest does not change in horizontal direction, but it changes in vertical direction where gravitational force acts. So, pressure increases as depth of the fluid increases, because more fluid rests on deeper levels, and effect of this "extra load" on a deeper level is balanced by an increase in pressure. Illustrated in (Fig 3.1). [7].

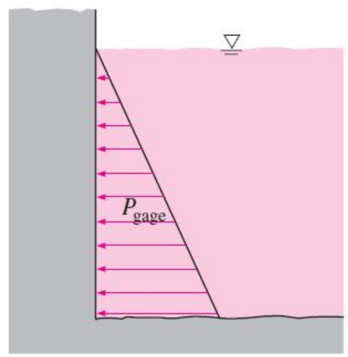

Fig. 3.1 Pressure of fluid at rest increases with depth

To obtain a relation for change in pressure with depth, let us assume a rectangular fluid element of height Δz, length Δx and unit depth in equilibrium, as illustrated in (Fig 3.2). Considering density of the fluid ρ to be constant, a force balance in vertical z-direction gives

$$\Sigma F_z = ma_z = 0; P_2\Delta x - P_1\Delta x - \rho g\Delta x\Delta z = 0, \qquad \text{(Eq. 3.1)}$$

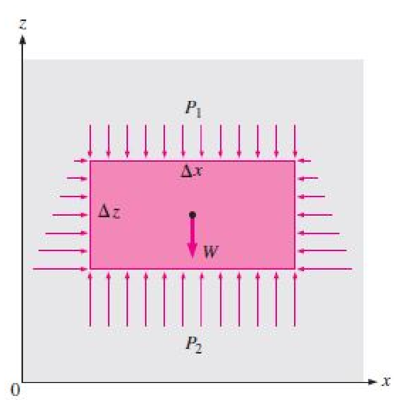

Fig. 3.2 Free body diagram of rectangular fluid element in equilibrium

where $W = mg = \rho g\, \Delta x\, \Delta z$ is the weight of the fluid element.
Dividing by Δx and rearranging gives

$$\Delta P = P_2 - P_1 = \rho g \Delta z = \gamma s \Delta z, \qquad \text{(Eq. 3.2)}$$

where $\gamma_s = \rho g$ is the *specific weight* of the fluid.
Thus, we conclude that the pressure difference between two points in a constant density fluid is proportional to the vertical distance Δz between the points and the density ρ of the fluid. In other words, pressure in a fluid increases linearly with depth.

4. 3D- DESIGN OF SEAWEED CULTIVATION MODULE

Design of seaweed cultivation module. Its dimensions are (L × W × H) 5980×4082×5418 mm excluding bottom ropes. As the module is axis symmetry only half sections are considered.

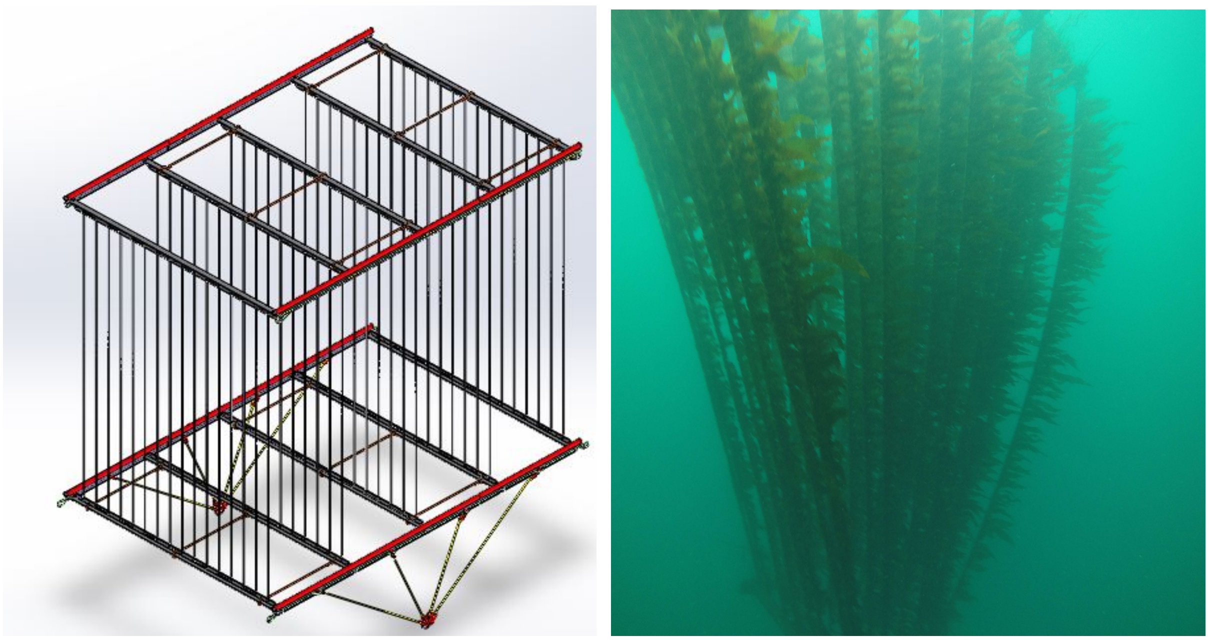

Fig. 4.1 Isometric view

Let us see how hydrostatic pressure acts on the module and due to this hydrostatic pressure, stress and displacement occurred on module. For analyzing the effect of hydrostatic pressure and calculating stress and displacement, we used Solidworks Simulation.

4.1. Half Structure

The 3D model of the half structure is presented in Fig. 4.2.

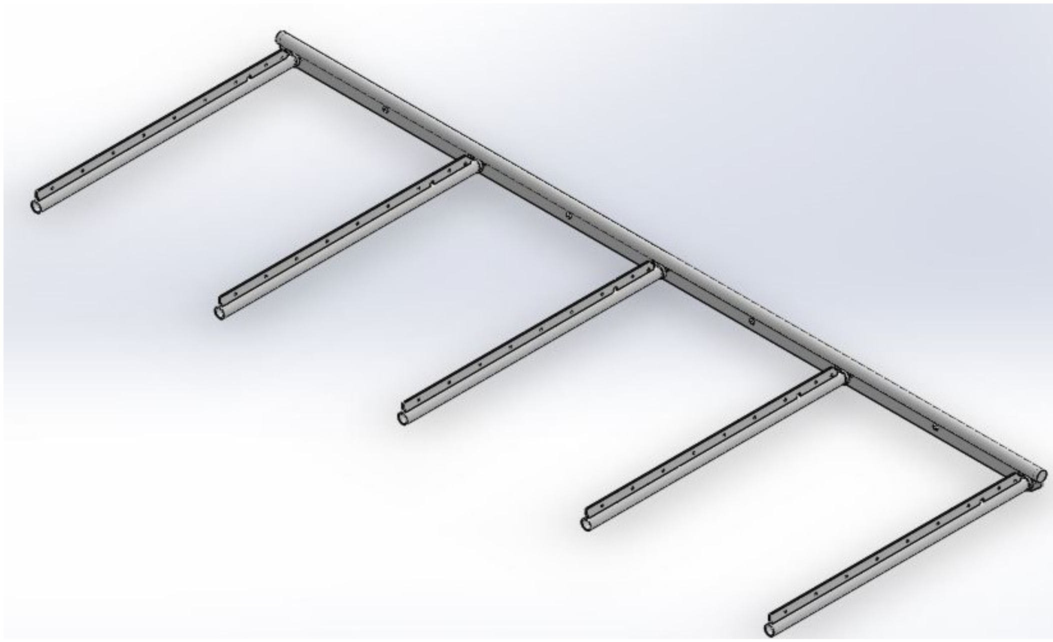

Fig. 4.2 Isometric view of half structure

4.1.1. Applied Fixtures

a) Reference geometry fixture is considered and applied on the holes with reference to top plane and displacement is allowed in Y- direction which is normal to plane (see Fig. 4.3).

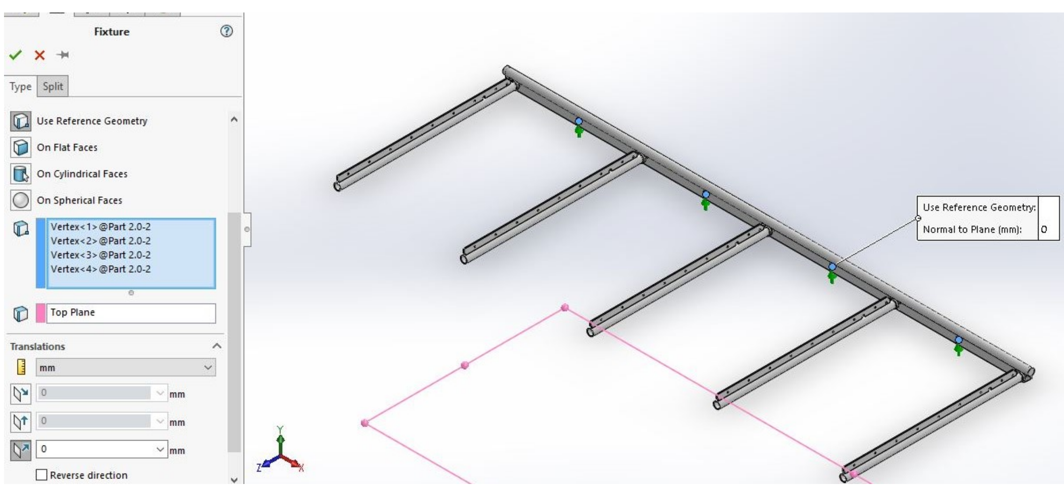

Fig. 4.3 Reference geometry fixture

b) Roller slider fixture is considered and applied on the side face of the module so that it can slide (see Fig. 4.4).

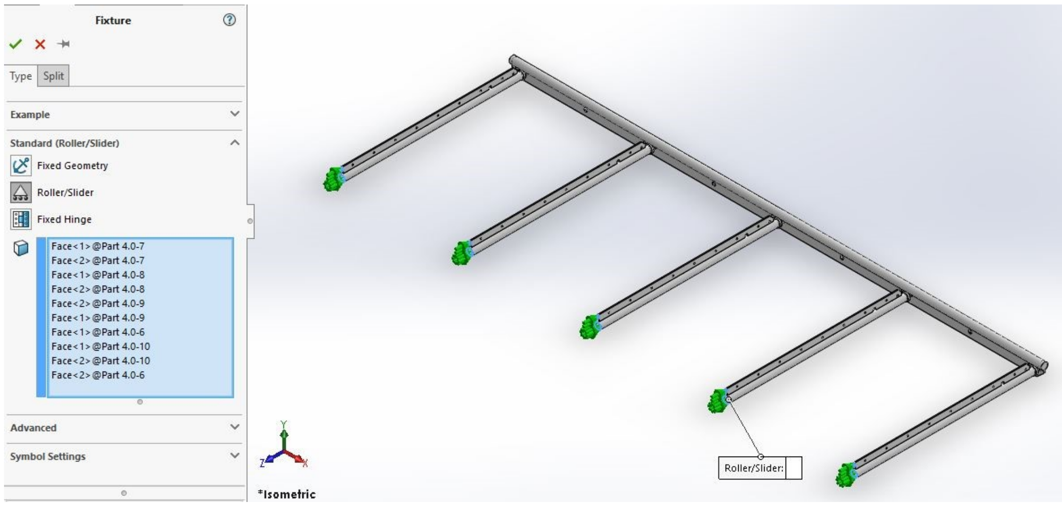

Fig. 4.4 Roller Slider fixture

c) Reference geometry fixture is considered and applied on the edge with adjacent face and displacement is allowed in X- direction which is normal to plane (see Fig. 4.5).

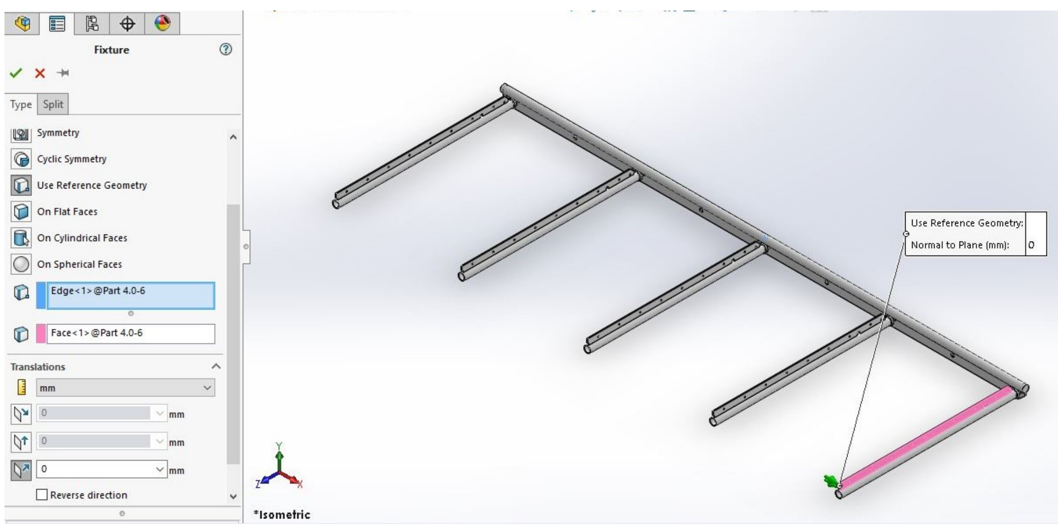

Fig. 4.5 Reference geometry fixture

4.1.2. Meshing of structure

Very fine mesh is applied to the structure taking into consideration of holes and extrude cut in the module (see Fig. 4.6).

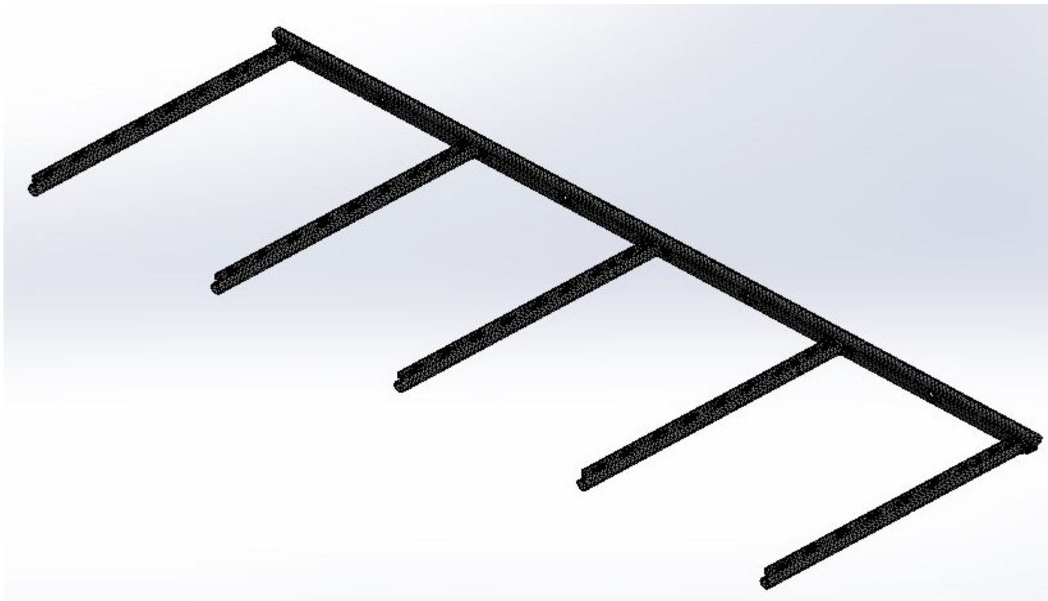

Fig. 4.6 Meshing done for the structure

4.1.3. Loads Applied and Results

a) Gravity

Load due to gravitational force is considered and applied (see Fig. 4.7).

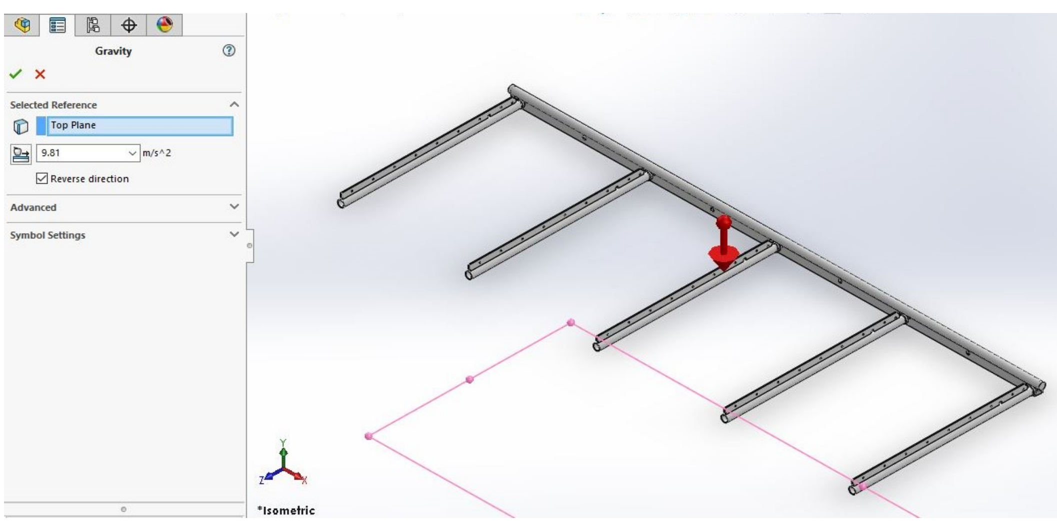

Fig. 4.7 Load due to gravity

Stress induced due to gravity on the module is represented below. Maximum stress induced is 2.834 MPa (see Fig. 4.8).

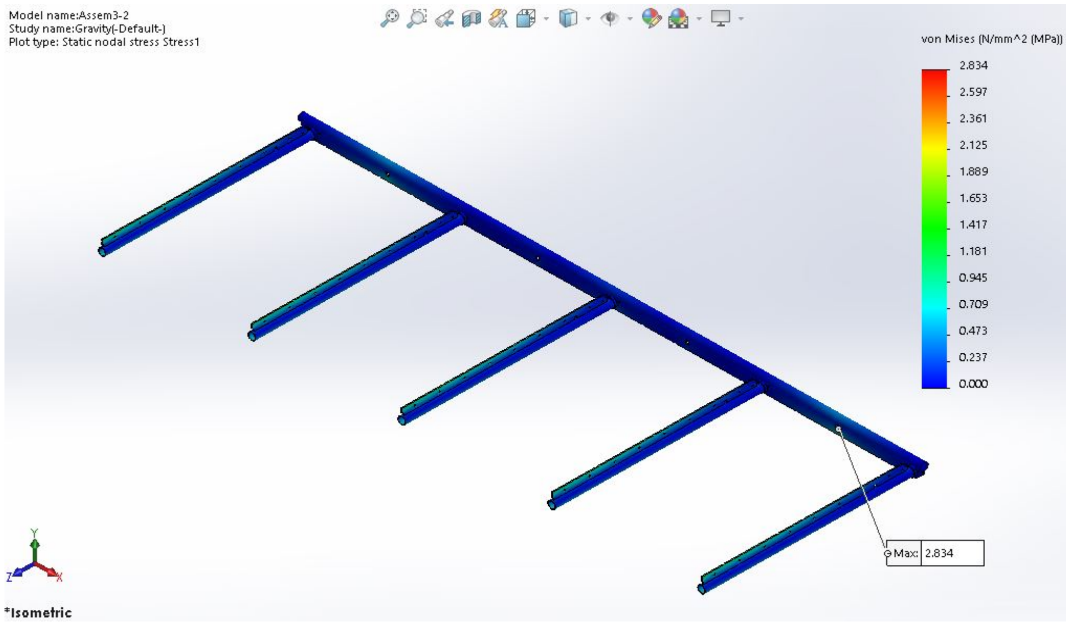

Fig. 4.8 Stress by gravitational force

Displacement due to gravitational force is represented below. Maximum displacement is 33.129 mm (see Fig. 4.9).

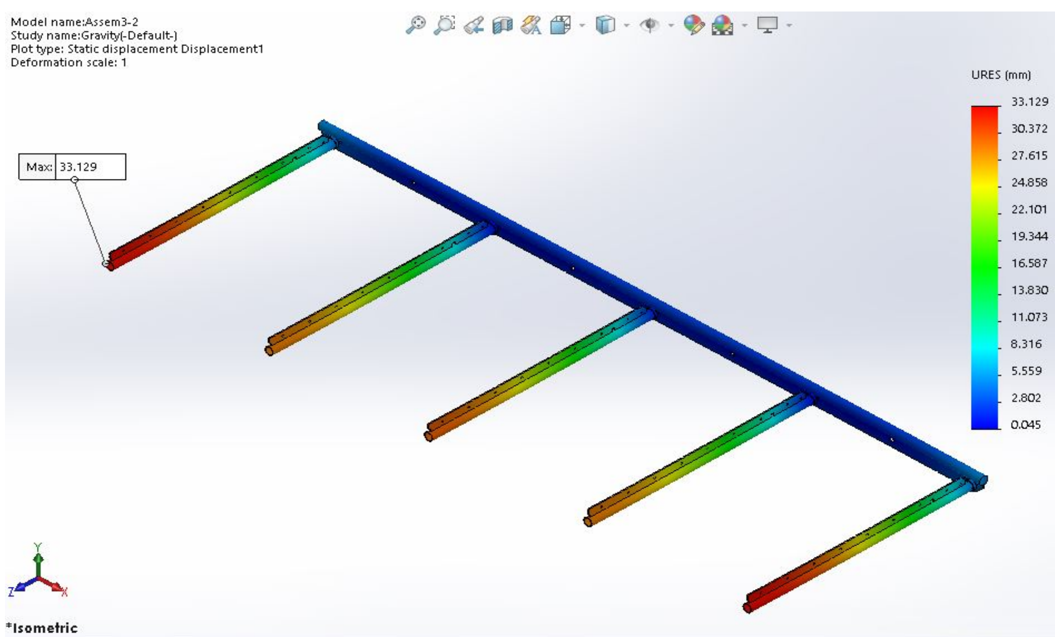

Fig. 4.9 Displacement by gravitational force

b) 0 metre depth

Loads applied: Load due to gravitational force is considered and applied (see Fig. 4.10).

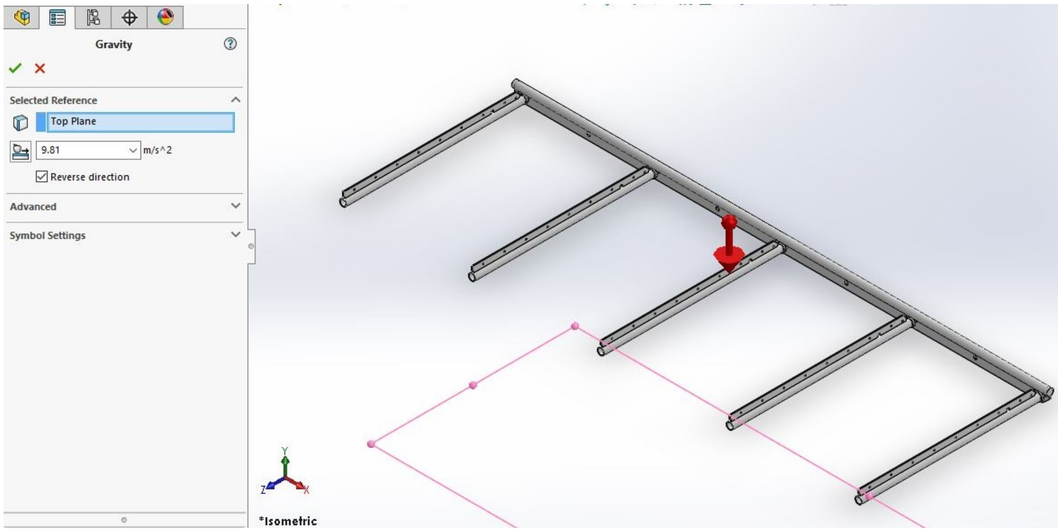

Fig. 4.10 Load due to gravity

Hydrostatic pressure load is considered and applied on the selected faces of structure (see Fig. 4.11).

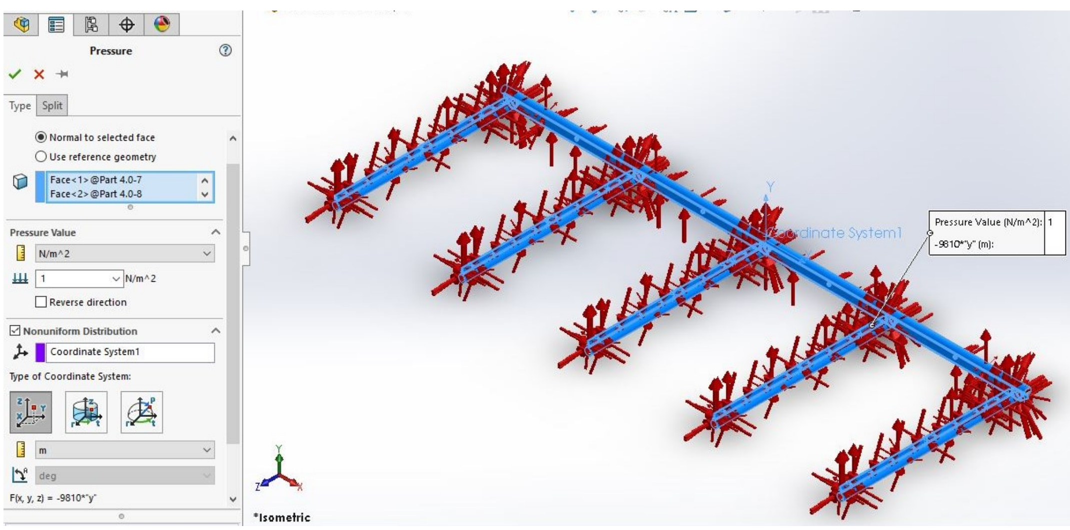

Fig. 4.11 Hydrostatic pressure for 0 m depth

Pressure load at 0 m can be calculated as per (Eq. 3.2).

$\Delta P = \rho g \Delta z = 9.81 \cdot 1000 \cdot 0 = 0$ MPa.

Stress induced due at 0 m depth on the module is represented below. Maximum stress induced is 3.813 MPa (see Fig. 4.12).

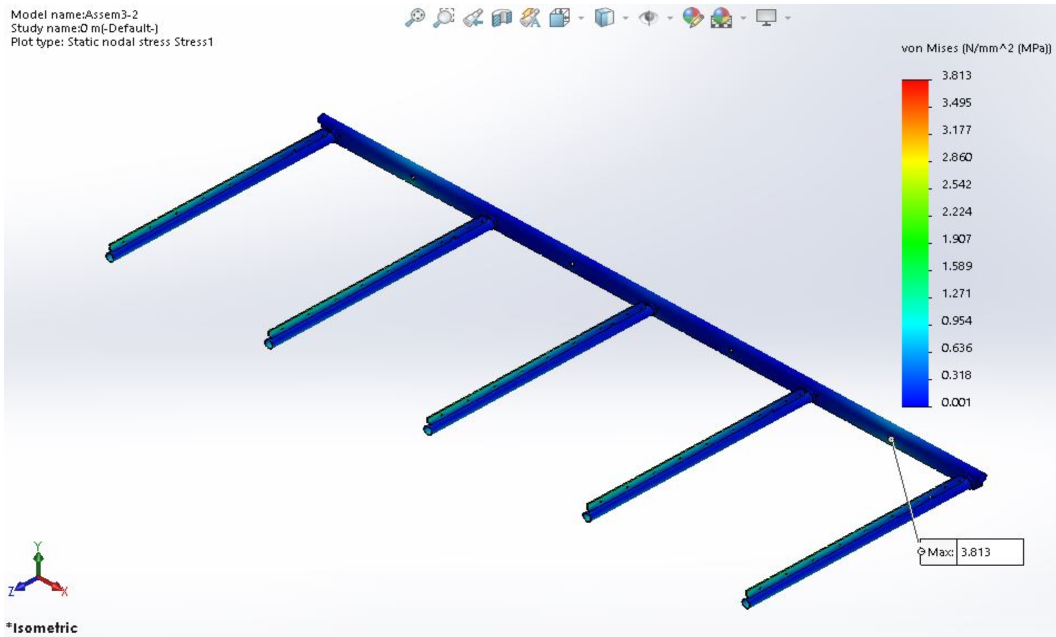

Fig. 4.12 Stress induced at 0 m depth

Displacement at 0 m depth is represented below. Maximum displacement is 48.22 mm (see Fig. 4.13).

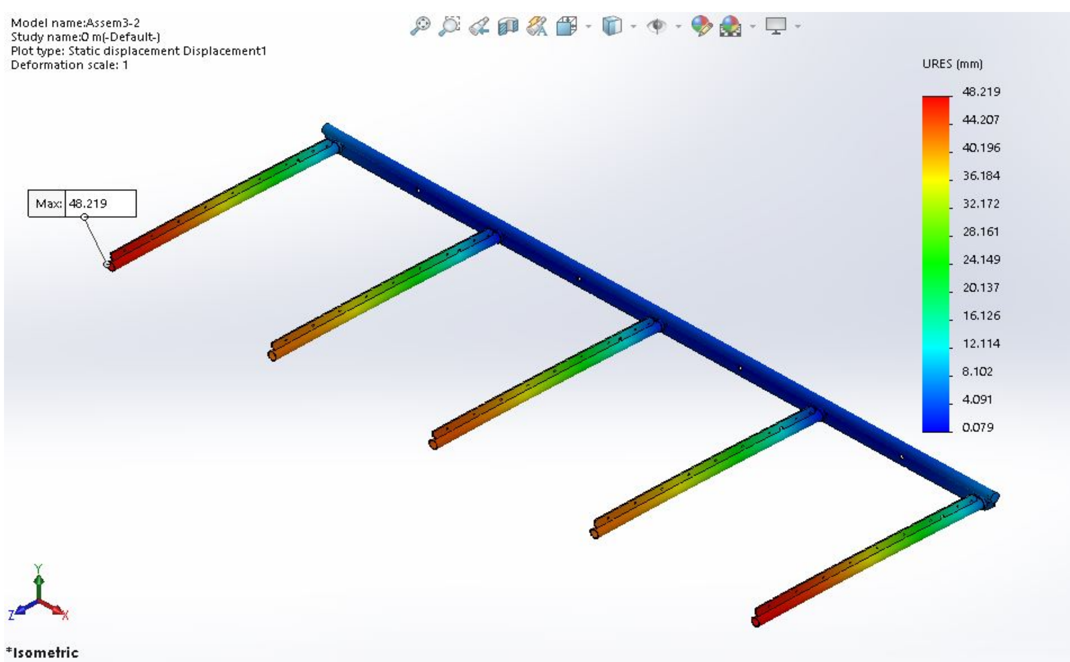

Fig. 4.13 Displacement at 0 m depth

c) 1, 10, 20 and 30 metre depth

Loads applied: Load due to gravitational force is considered and applied (see Fig. 4.14).

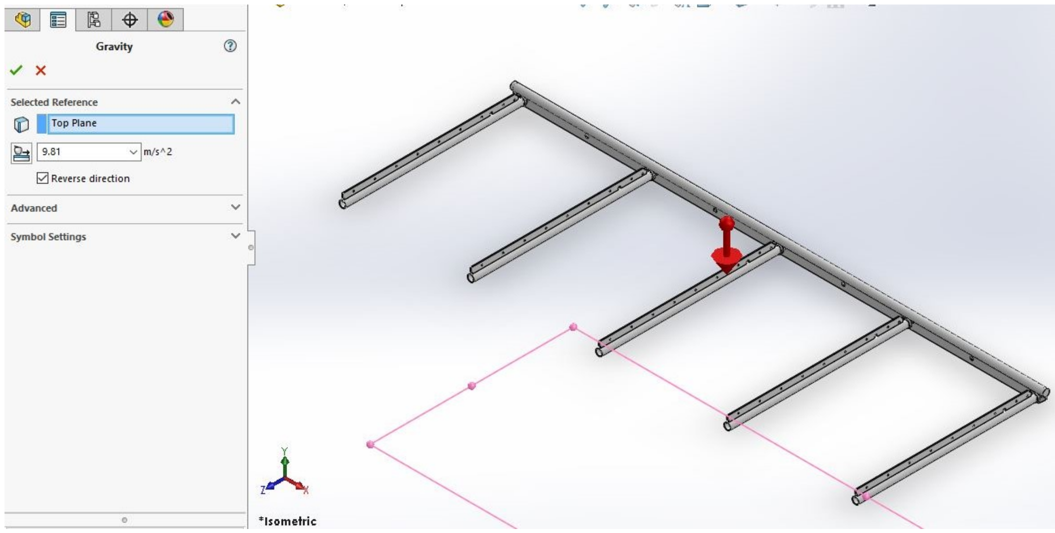

Fig. 4.14 Load due to gravity

Hydrostatic pressure load is considered and applied on the selected faces of structure (see Fig. 4.15).

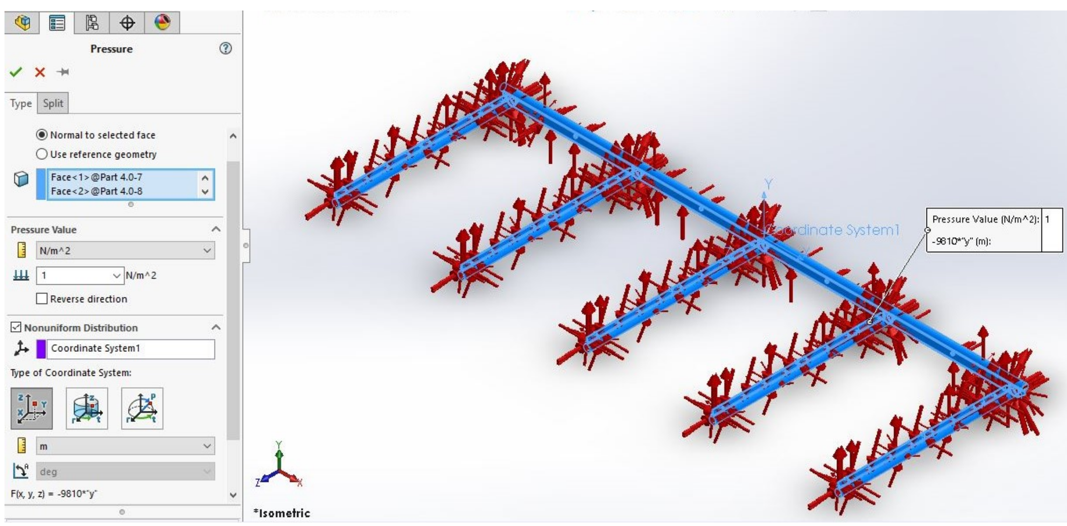

Fig. 4.15 Hydrostatic pressure for 1 m depth

Pressure load at 1 m can be calculated as per (Eq. 3.2)

$\Delta P = \rho g \Delta z \; = 9.81 \cdot 1000 \cdot 1 = 9810$ MPa.

Pressure load at 10 m can be calculated as per (Eq. 3.2)

$\Delta P = \rho g \Delta z \; = 9.81 \cdot 1000 \cdot 10 = 98100$ MPa

Pressure load at 20 m can be calculated as per (Eq. 3.2)

$\Delta P = \rho g \Delta z \; = 9.81 \cdot 1000 \cdot 20 = 196200$ MPa

Pressure load at 30 m can be calculated as per (Eq. 3.2)

$\Delta P = \rho g \Delta z \; = 9.81 \cdot 1000 \cdot 30 = 294300$ MPa

Pressure load at 1, 10, 20 and 30 m depth is considered and applied on the selected faces of structure (see Fig. 4.16).

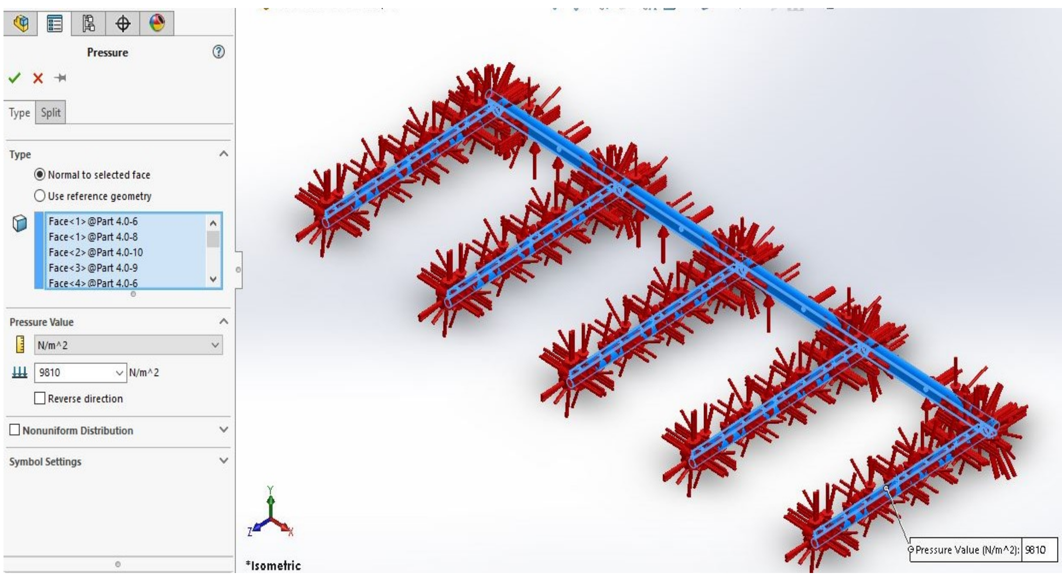

Fig. 4.16 Pressure load at 1, 10, 20 and 30 m depth

Stress induced at 1 m depth on the module is represented below. Maximum stress induced is 3.779 MPa (see Fig. 4.17).

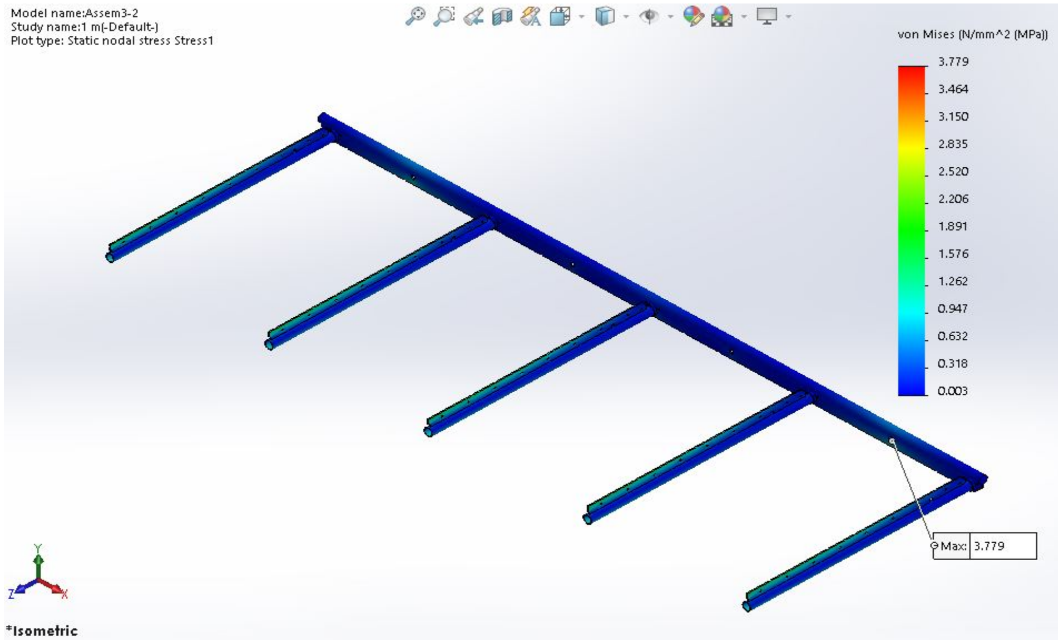

Fig. 4.17 Stress induced at 1 m depth

Displacement at 1 m depth is represented below. Maximum displacement is 48.6 mm (see Fig. 4.18).

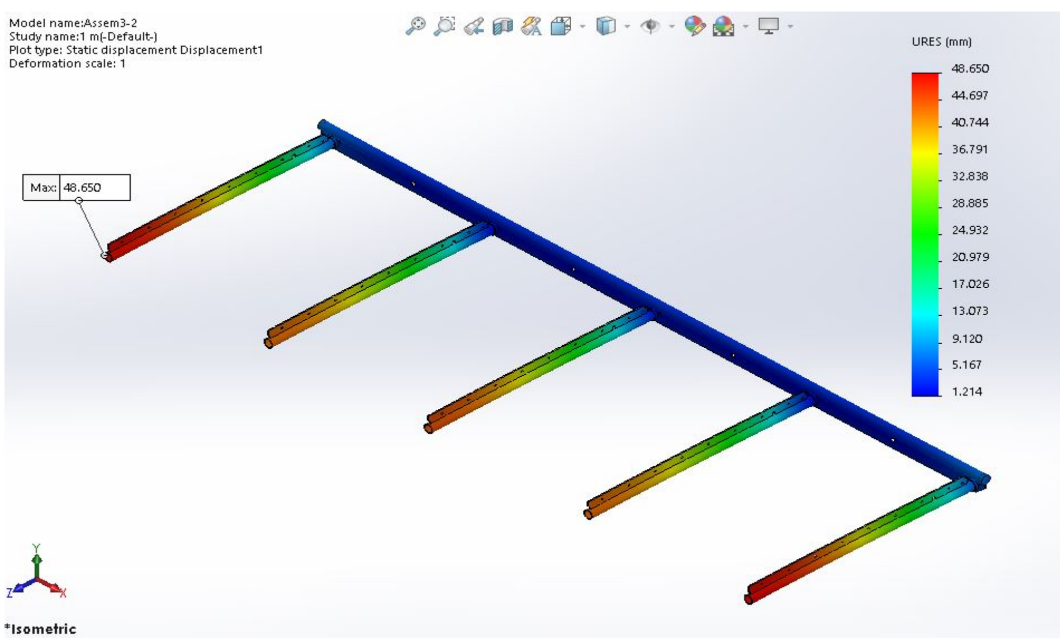

Fig. 4.18 Displacement at 1 m depth

d) 10 metre depth

Stress induced at 10 m depth on the module is represented below. Maximum stress induced is 3.483 MPa (see Fig. 4.19).

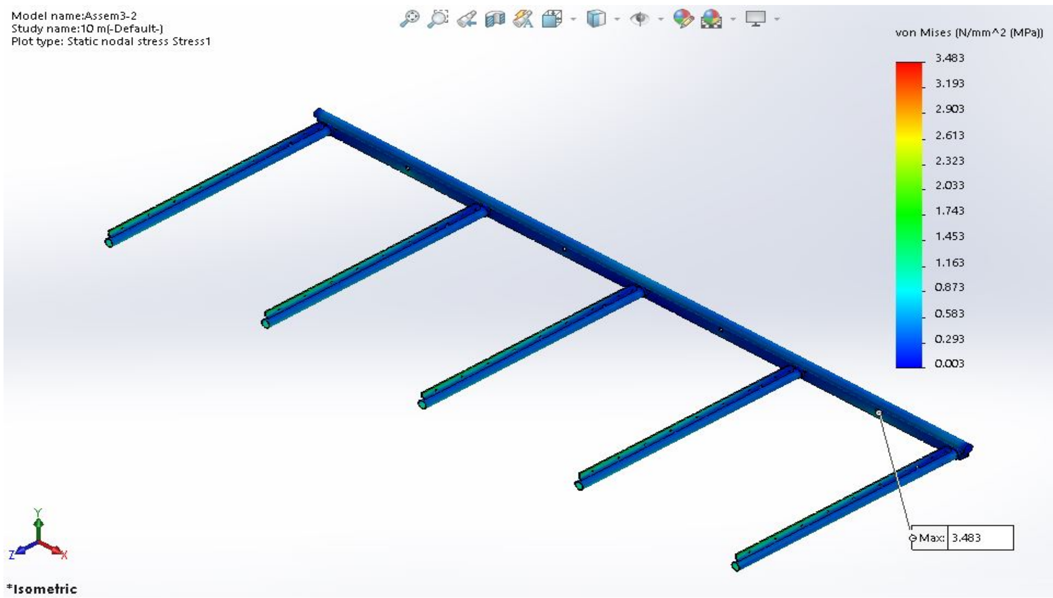

Fig. 4.19 Stress induced at 10 m depth

Displacement at 10 m depth is represented below. Maximum displacement is 54.105 mm (see Fig. 4.20).

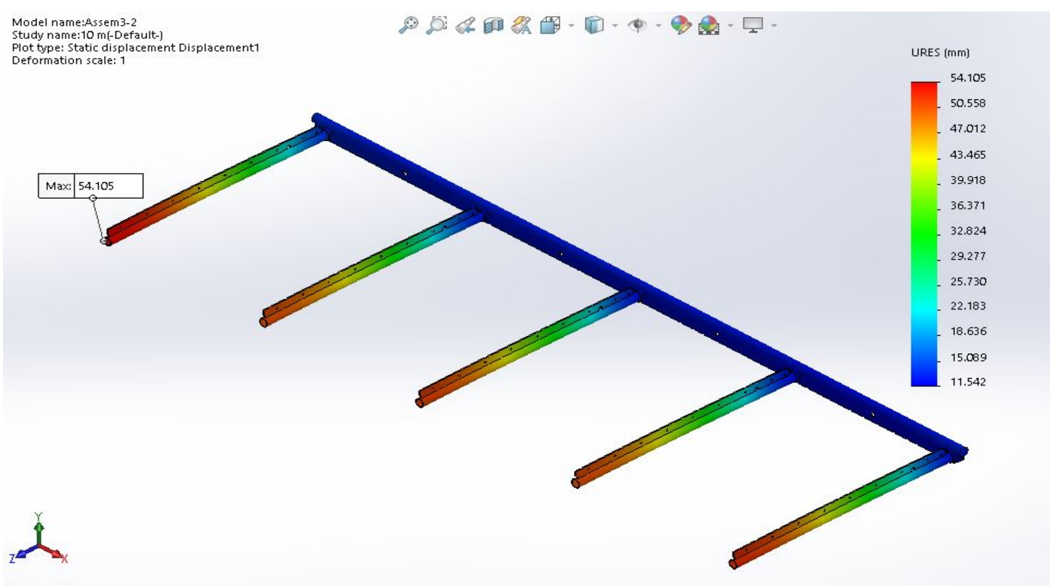

Fig. 4.20 Displacement at 10 m depth

e) 20 metre depth

Stress induced at 20 m depth on the module is represented below. Maximum stress induced is 3.157 MPa (see Fig. 4.21).

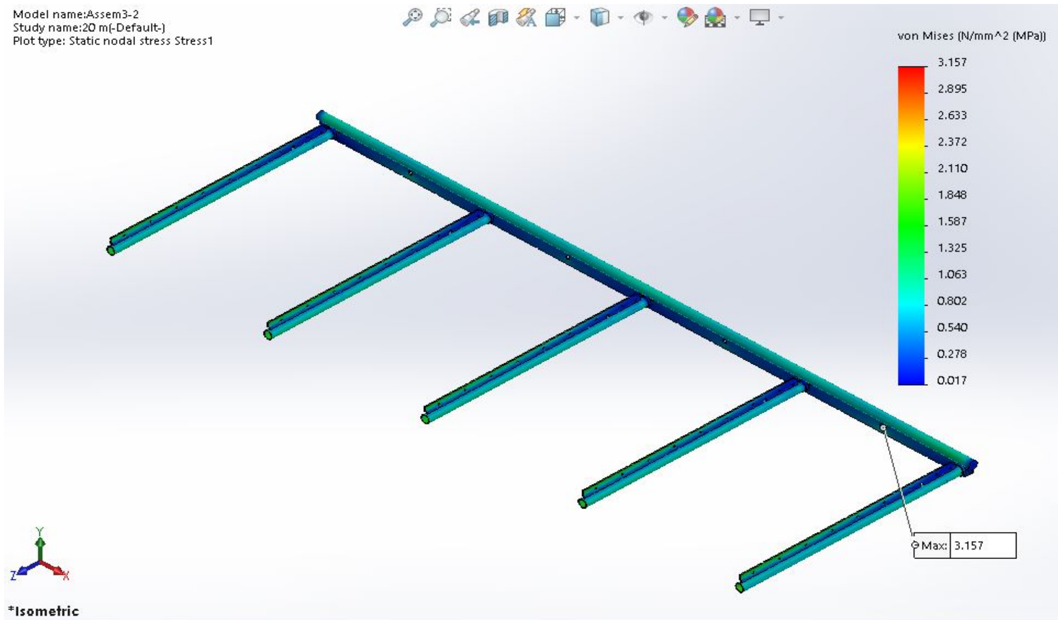

Fig. 4.21 Stress induced at 20 m depth

Displacement at 20 m depth is represented below. Maximum displacement is 62.654 mm (see Fig. 4.22).

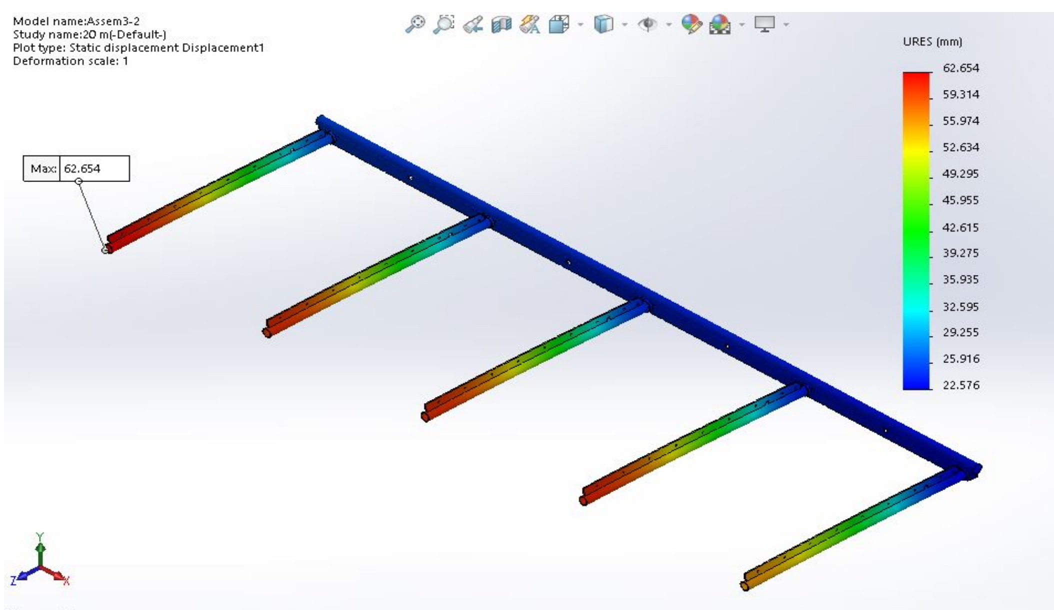

Fig. 4.22 Displacement at 20 m depth

f) 30 metre depth

Stress induced at 30 m depth on the module is represented below. Maximum stress induced is 2.948 MPa (see Fig. 4.23).

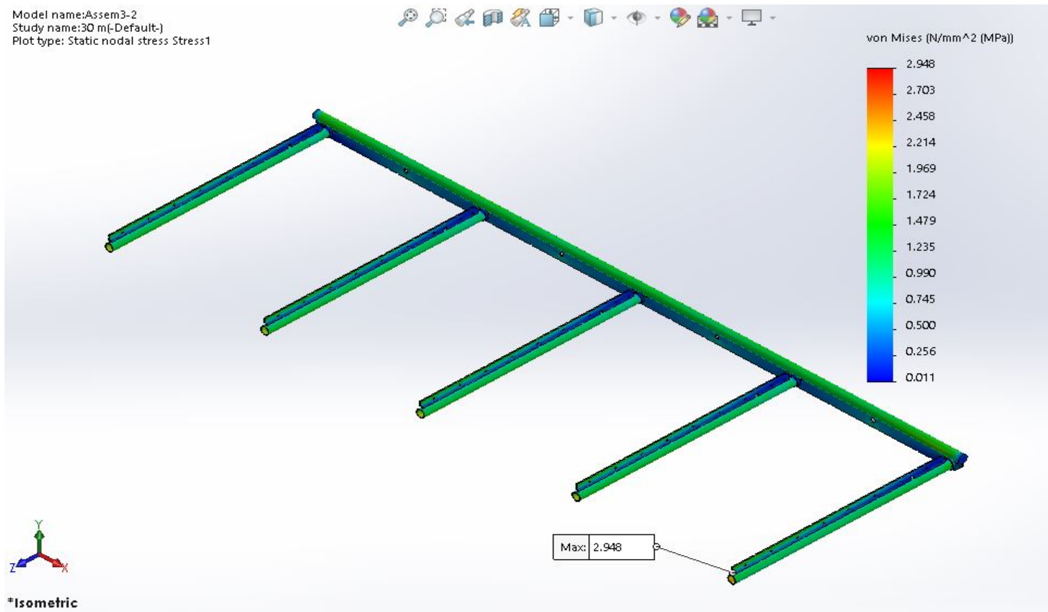

Fig. 4.23 Stress induced at 30 m depth

Displacement at 30 m depth is represented below. Maximum displacement is 73.214 mm (see Fig. 4.24).

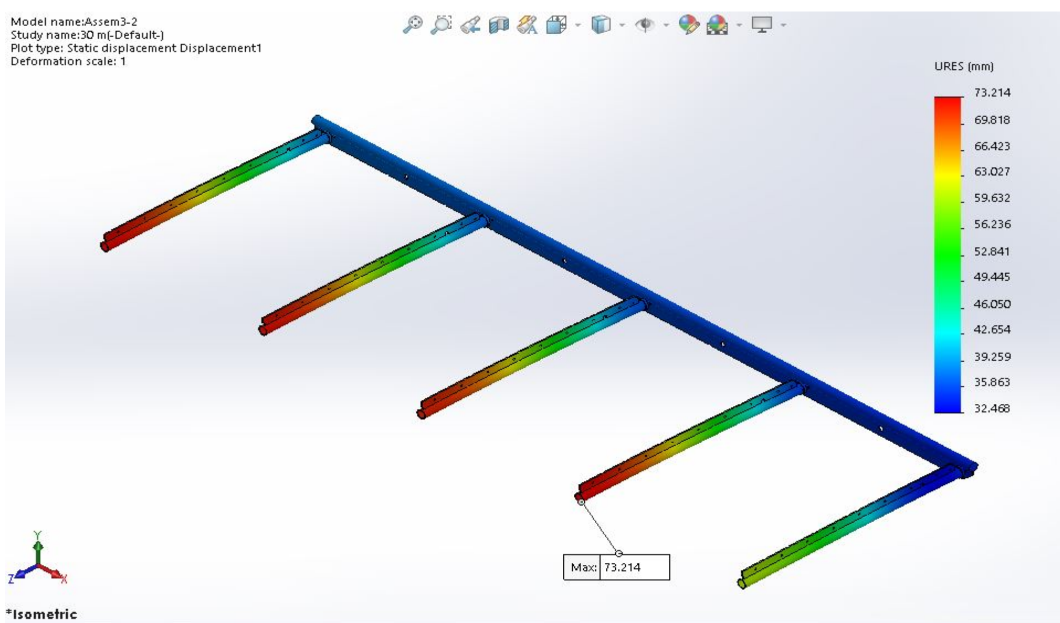

Fig. 4.24 Stress induced at 30 m depth

4.2. Whole Structure

The 3D model of the half structure is presented in Fig. 4.25.

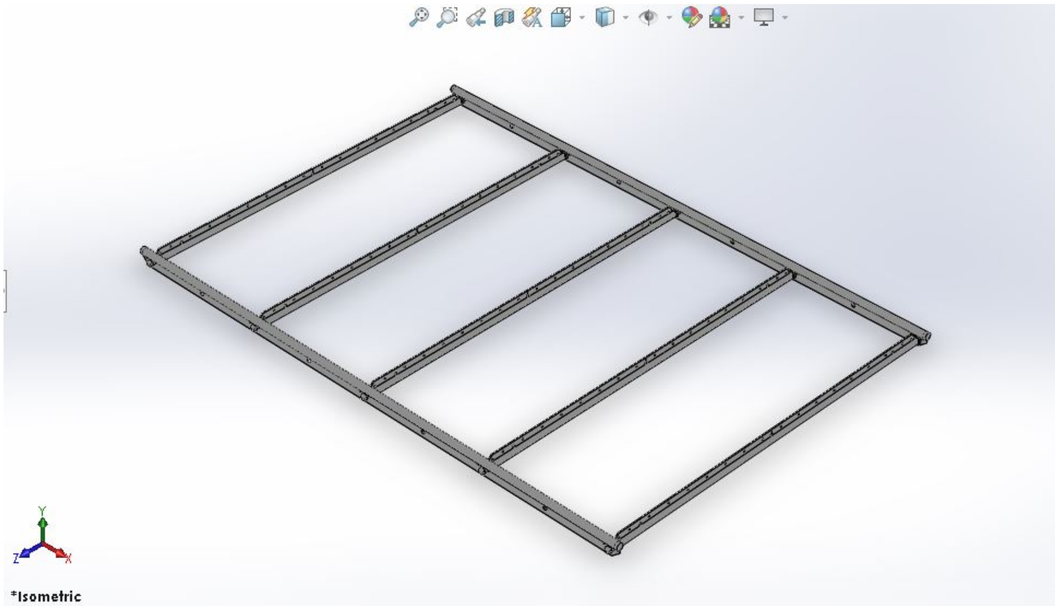

Fig. 4.25 Isometric view of Whole Structure

4.2.1. Applied Fixtures

a) Reference geometry fixture is considered and applied on the holes with reference to top plane and displacement is allowed in Y- direction which is normal to plane (see Fig. 4.26)

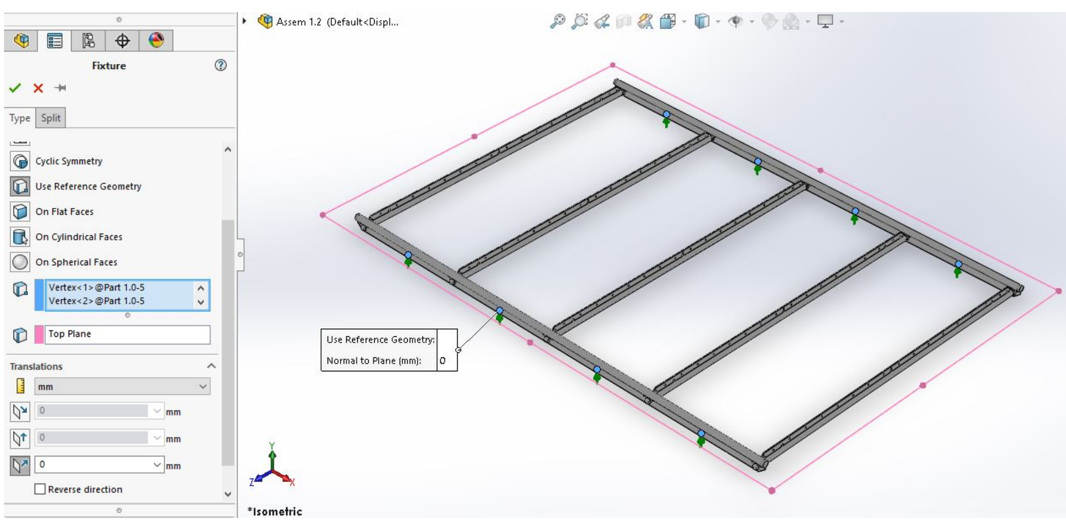

Fig. 4.26 Reference geometry fixture

b) Roller slider fixture is considered and applied on the holes were structure is allowed to slide (see Fig. 4.27).

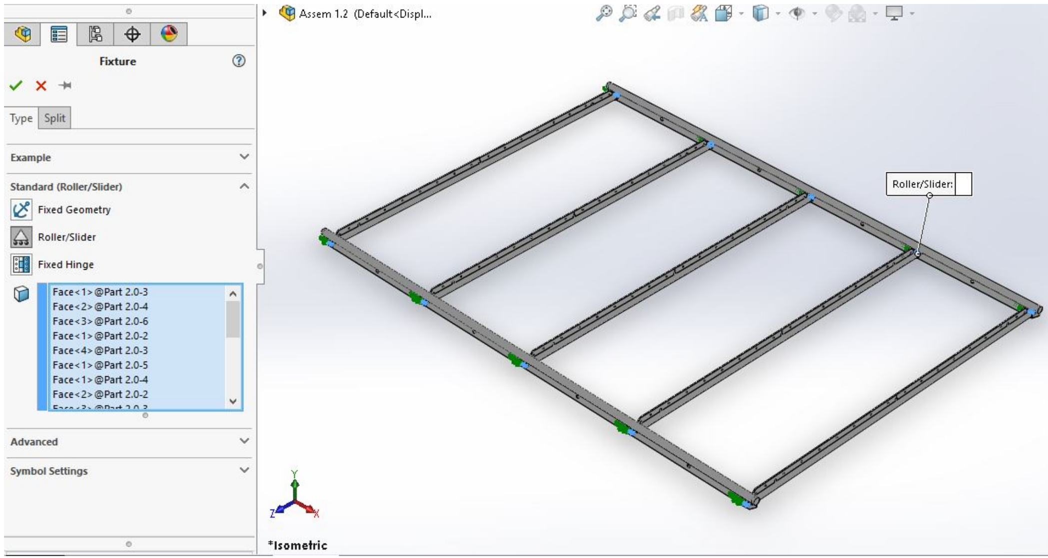

Fig. 4.27 Roller Slider fixture

c) Reference geometry fixture is considered and applied on the two faces with reference to top plane and displacement is allowed in X and Y- direction which is normal to plane (see Fig. 4.28).

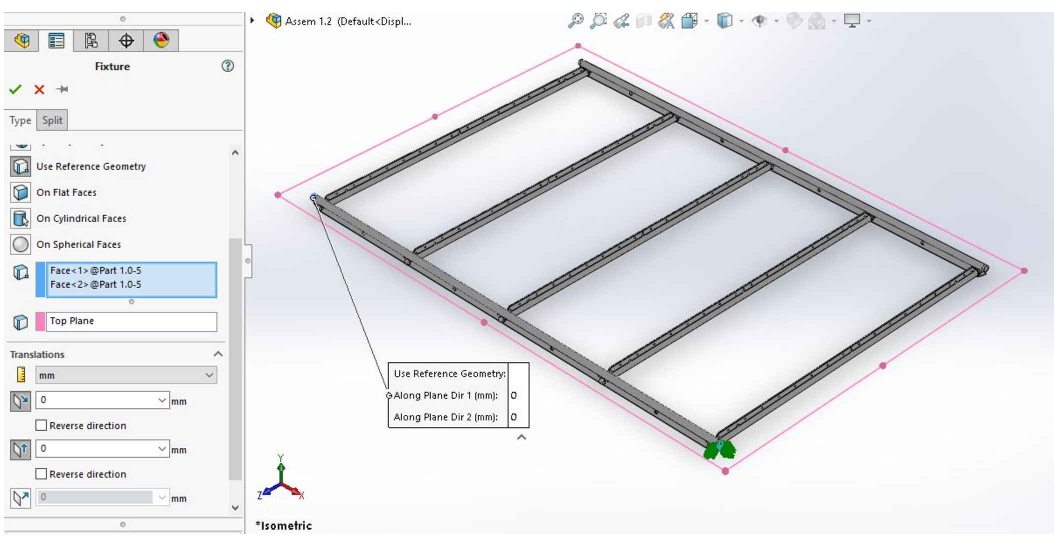

Fig. 4.28 Reference geometry fixture

d) Reference geometry fixture is considered and applied on the two faces with reference to top plane and displacement is allowed in X and Y- direction which is normal to plane (see Fig. 4.29).

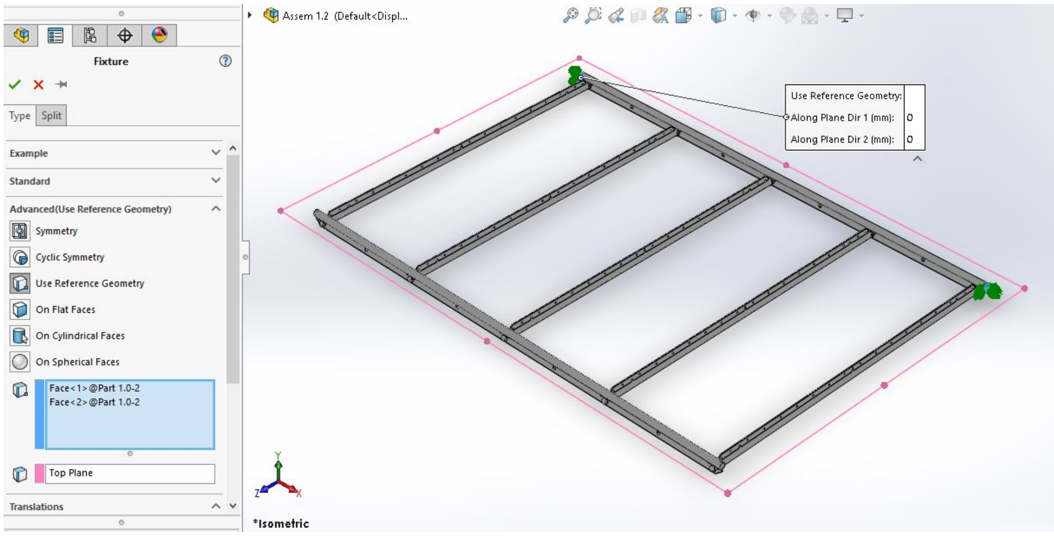

Fig. 4.29 Reference geometry fixture

4.2.2. Meshing of structure

Very fine mesh is applied to the structure and mesh control is applied to some parts taking into consideration of holes and extrude cut in the module (see Fig. 4.30).

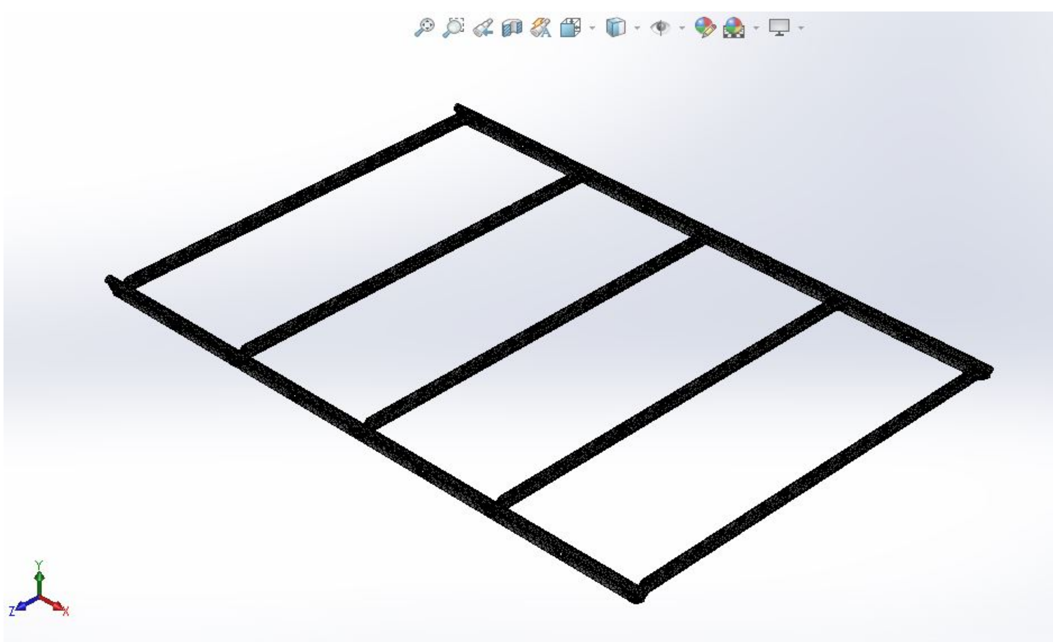

Fig. 4.30 Meshing done for the structure

4.2.3. Loads Applied and Results

a) Gravity

Load due to gravitational force is considered and applied (see Fig. 4.31).

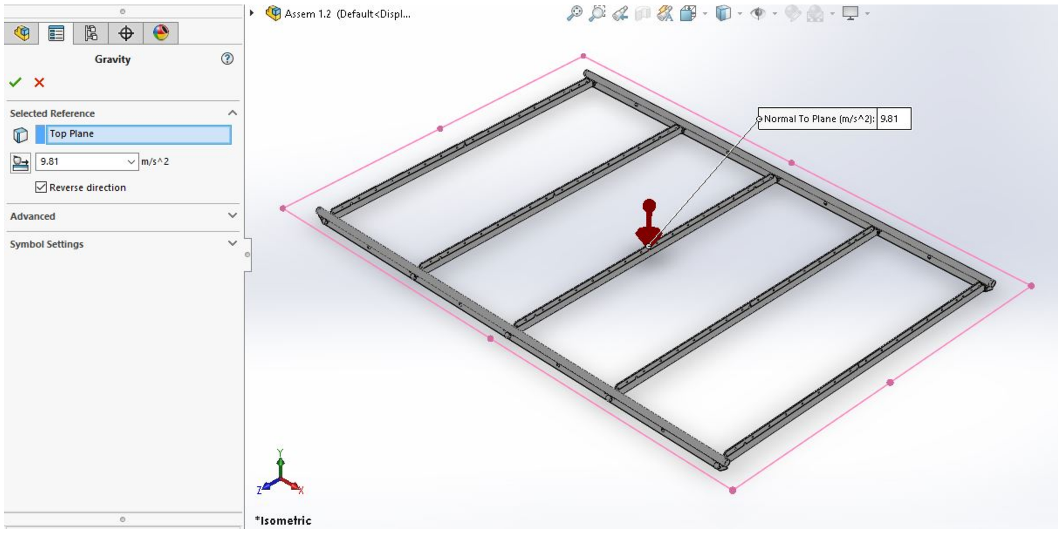

Fig. 4.31 Load due to gravity

Stress induced by gravitational force on the module is represented below. Maximum stress induced is 2.873 MPa (see Fig. 4.32).

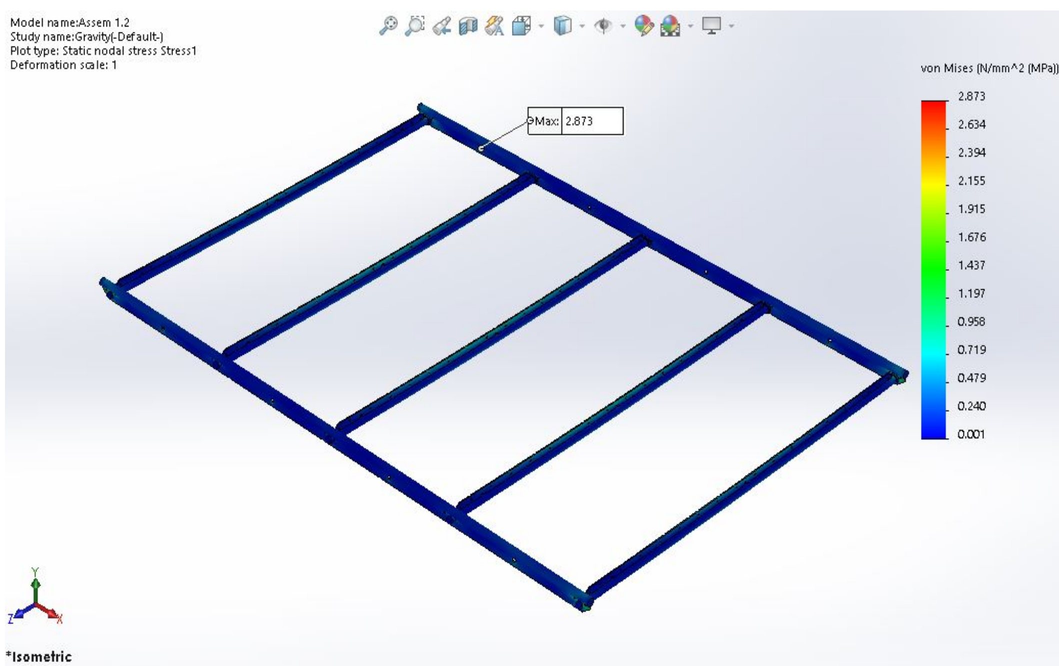

Fig. 4.32 Stress by gravitational force

Displacement due to gravitational force on the module is represented below. Maximum displacement is 27.799 mm (see Fig. 4.33).

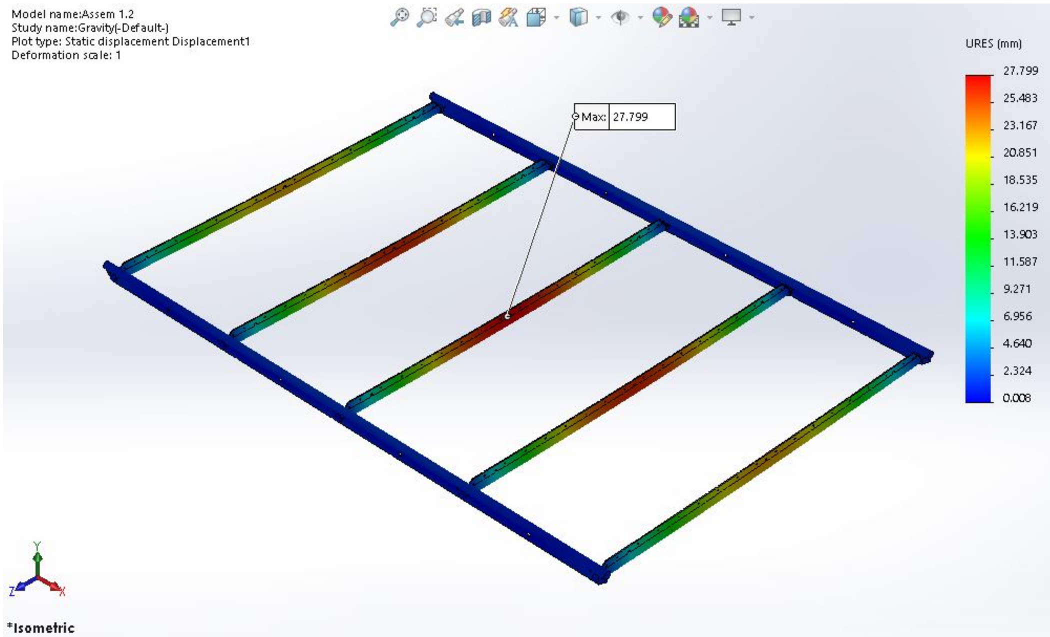

Fig. 4.33 Displacement by gravitational force

b) 0 metre depth

Loads applied: Gravitational force (see Fig. 4.34).

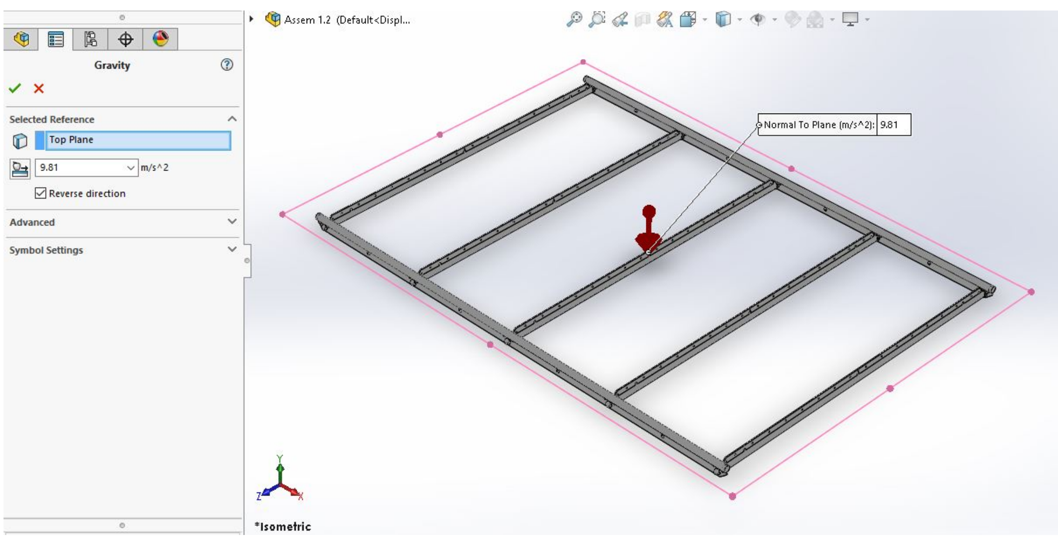

Fig. 4.34 Load due to gravity

Hydrostatic pressure load is considered and applied on the selected faces of structure (see Fig. 4.35).

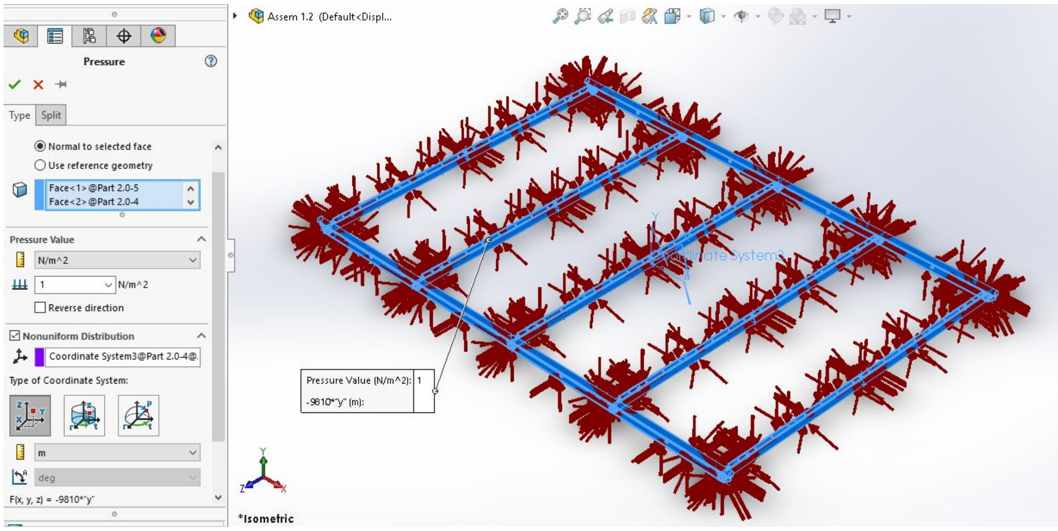

Fig. 4.35 Hydrostatic pressure for 0 m depth

Pressure load at 0 m depth can be calculated as per (Eq. 3.2)

$\Delta P = \rho g \Delta z = 9.81 \cdot 1000 \cdot 0 = 0$ MPa

Stress induced at 0 m depth on the module is represented below. Maximum stress induced is 3.945 MPa (see Fig. 4.36).

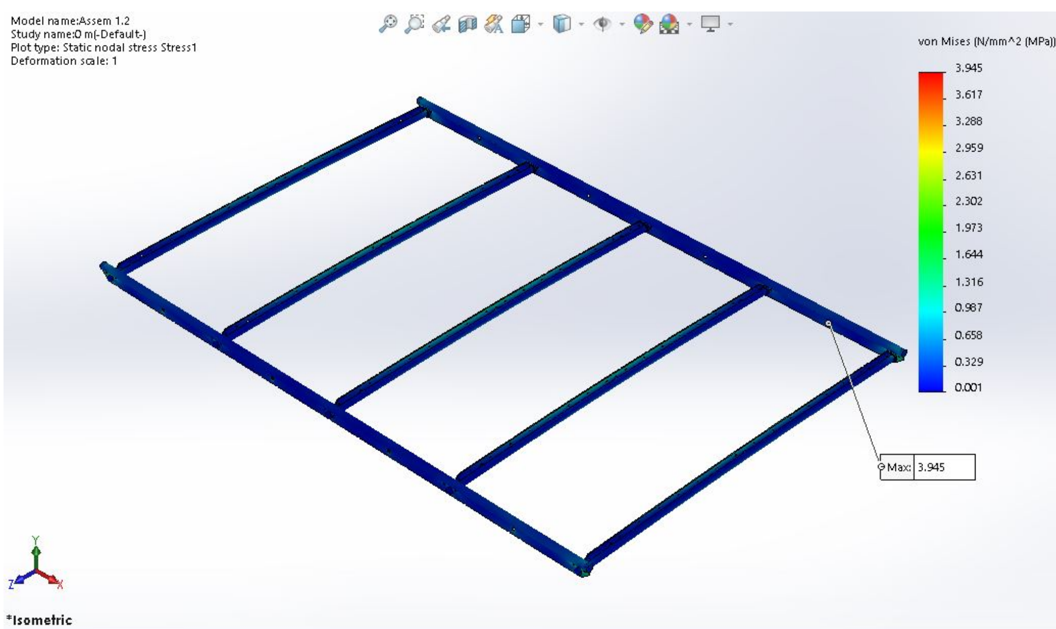

Fig. 4.36 Stress induced at 0 m depth

Displacement at 0 m depth on the module is represented below. Maximum displacement is 41.303 mm (see Fig. 4.37).

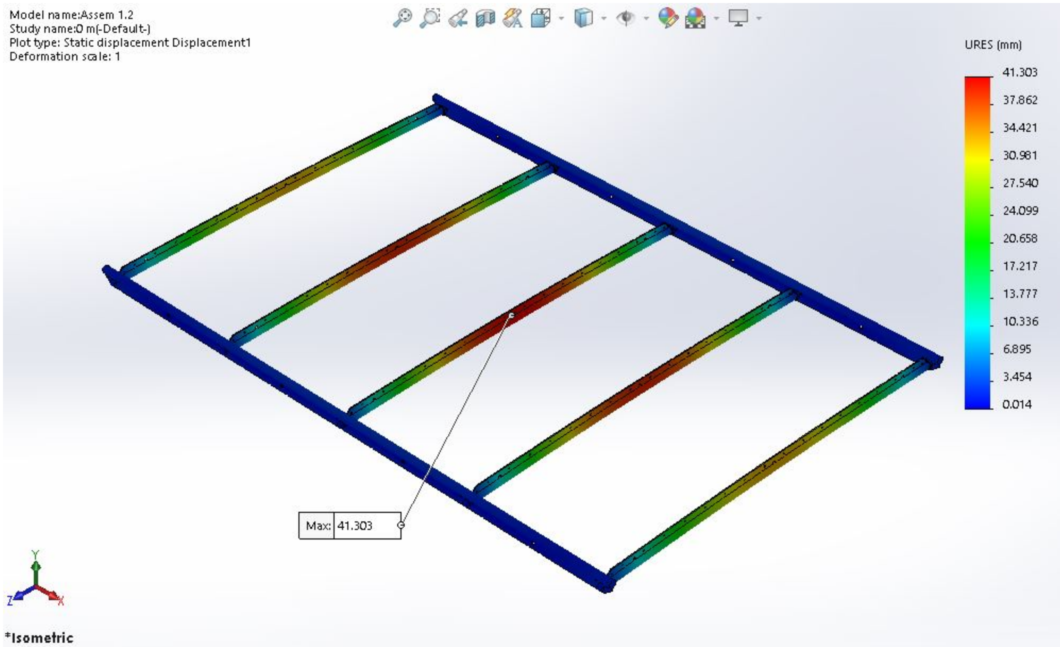

Fig. 4.37 Displacement at 0 m depth

c) 1, 10, 20, 30 metre depth

Loads applied: Load due to gravitational force is considered and applied (see Fig. 4.38).

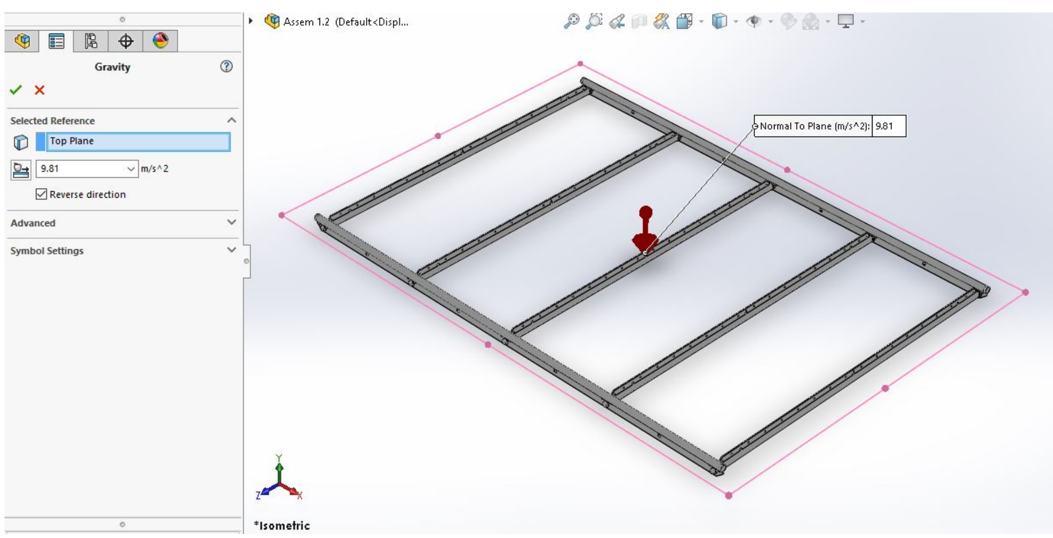

Fig. 4.38 Load due to gravity

Hydrostatic pressure load is considered and applied on the selected faces of structure (see Fig. 4.39).

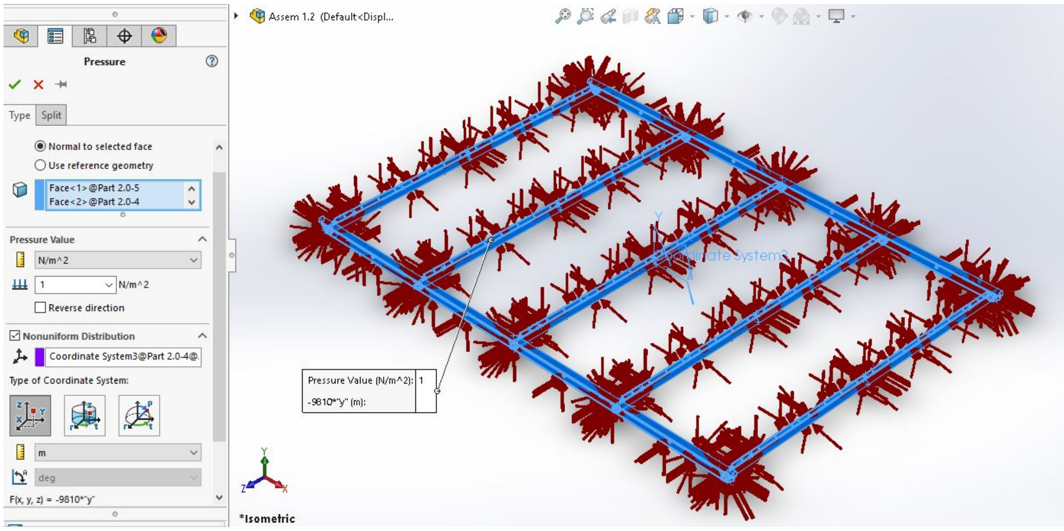

Fig. 4.39 Hydrostatic pressure for 1 m depth

Pressure load at 1 m can be calculated as per (Eq. 3.2)

$\Delta P = \rho g \Delta z = 9.81 \cdot 1000 \cdot 1 = 9810$ MPa.

Pressure load at 10 m can be calculated as per (Eq. 3.2)

$\Delta P = \rho g \Delta z = 9.81 \cdot 1000 \cdot 10 = 98100$ MPa

Pressure load at 20 m can be calculated as per (Eq. 3.2)

$\Delta P = \rho g \Delta z = 9.81 \cdot 1000 \cdot 20 = 196200$ MPa

Pressure load at 30 m can be calculated as per (Eq. 3.2)

$\Delta P = \rho g \Delta z = 9.81 \cdot 1000 \cdot 30 = 294300$ MPa

Pressure load at 1, 10, 20 and 30 m depth is considered and applied on the selected faces of structure (see Fig. 4.40).

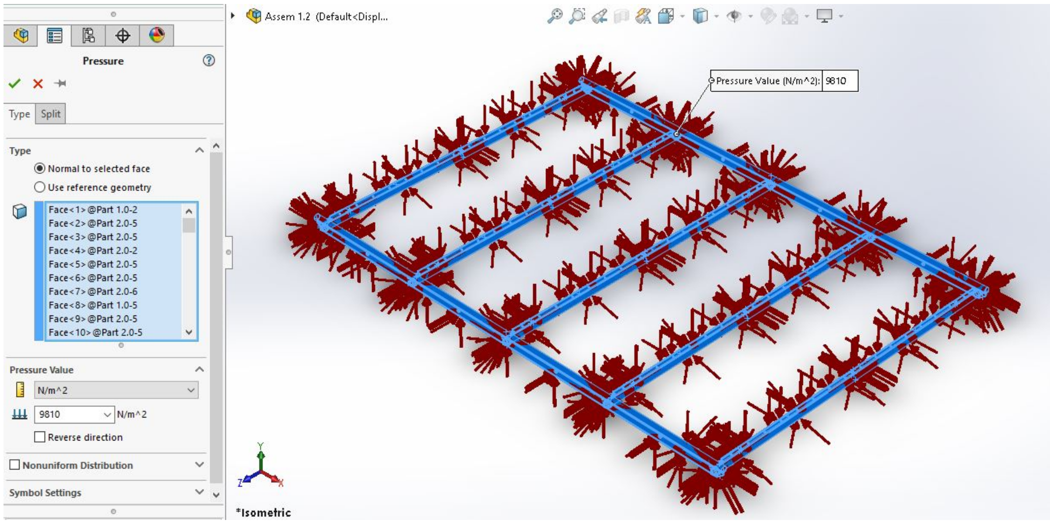

Fig. 4.40 Pressure load at 1, 10, 20 and 30 m depth

Stress induced at 1 m depth on the module is represented below. Maximum stress induced is 3.927 MPa (see Fig. 4.41).

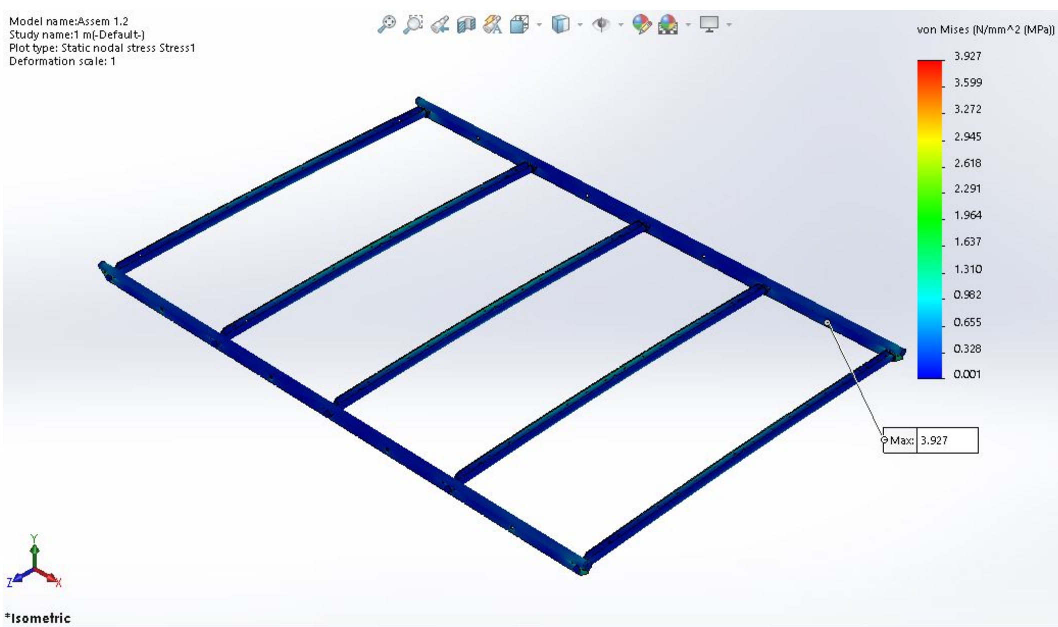

Fig. 4.41 Stress induced at 1 m depth

Displacement at 1 m depth on the module is represented below. Maximum displacement is 41.488 mm (see Fig. 4.42).

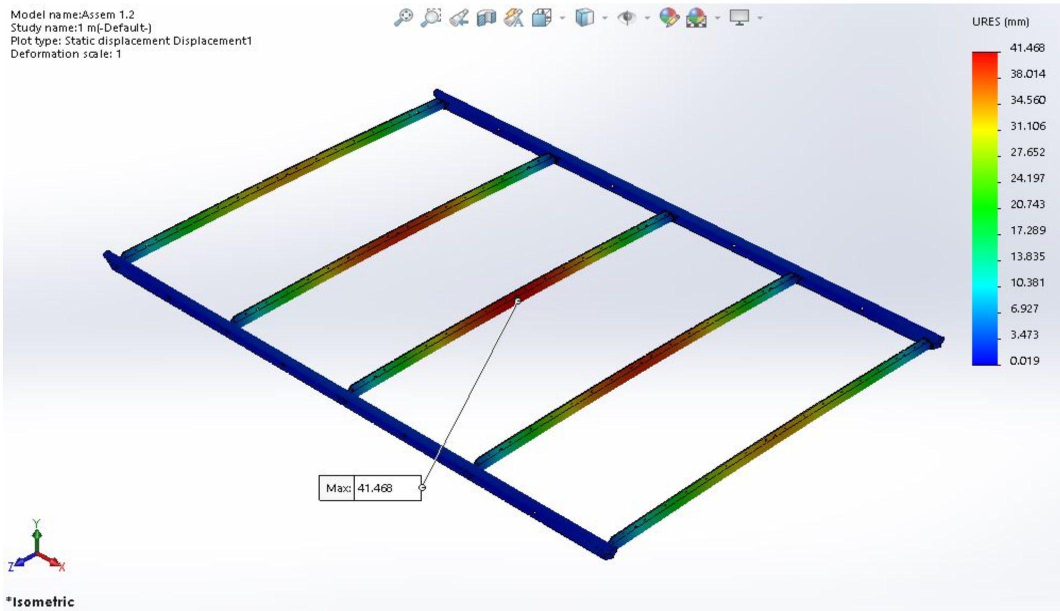

Fig. 4.42 Displacement at 1 m depth

d) 10 metre depth

Stress induced at 10 m depth on the module is represented below. Maximum stress induced is 3.770 MPa (see Fig. 4.43).

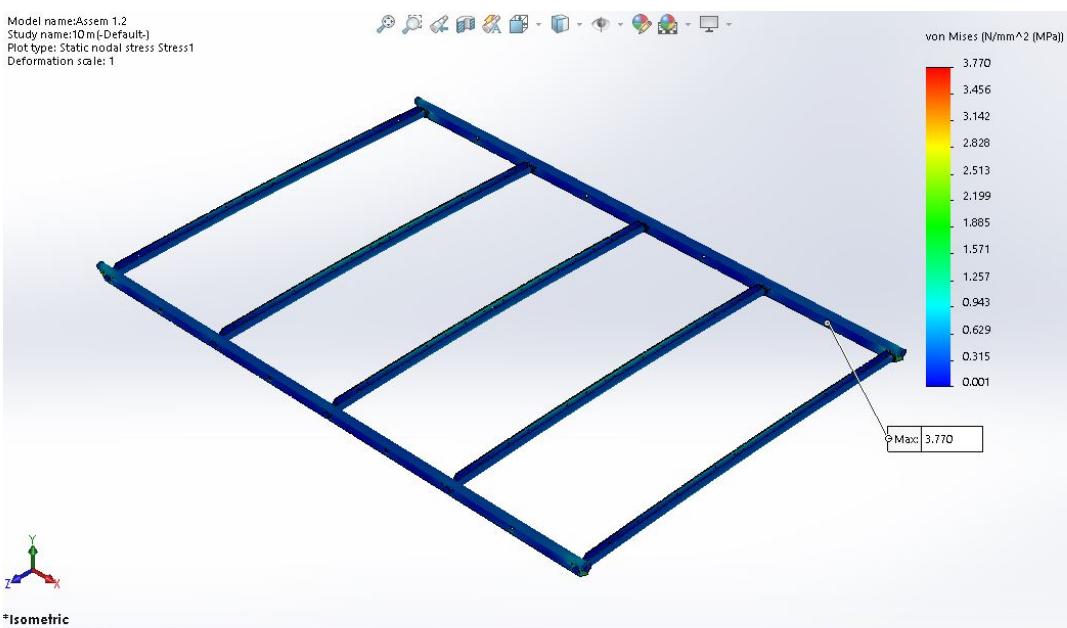

Fig. 4.43 Stress induced at 10 m depth

Displacement at 10 m depth on the module is represented below. Maximum displacement is 42.975 mm (see Fig. 4.44).

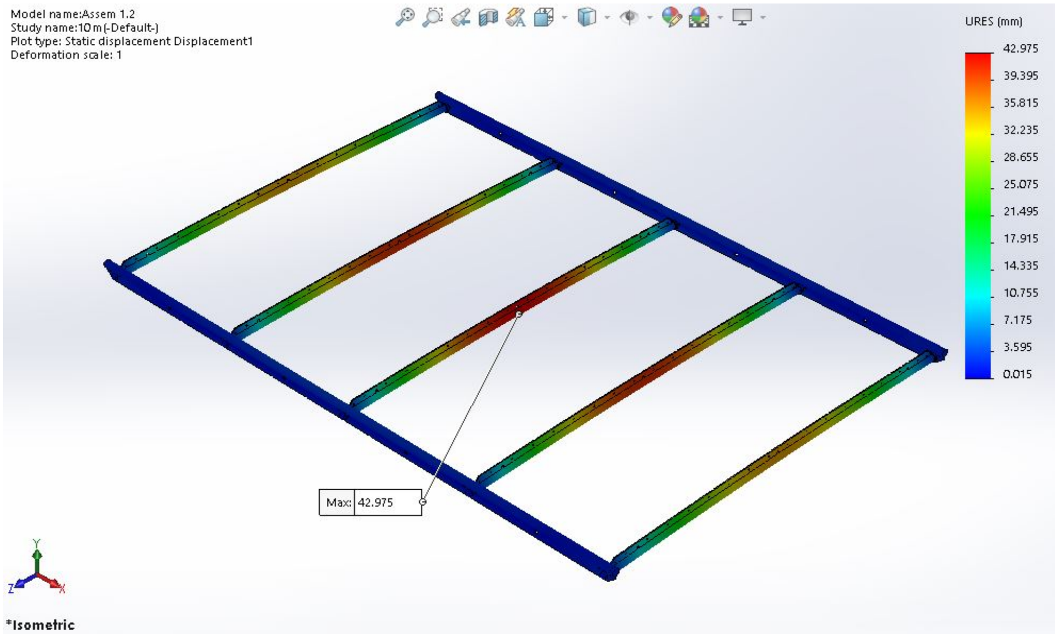

Fig. 4.44 Displacement at 10 m depth

e) 20 metre depth

Stress induced at 20 m depth on the module is represented below. Maximum stress induced is 4.068 MPa (see Fig. 4.45).

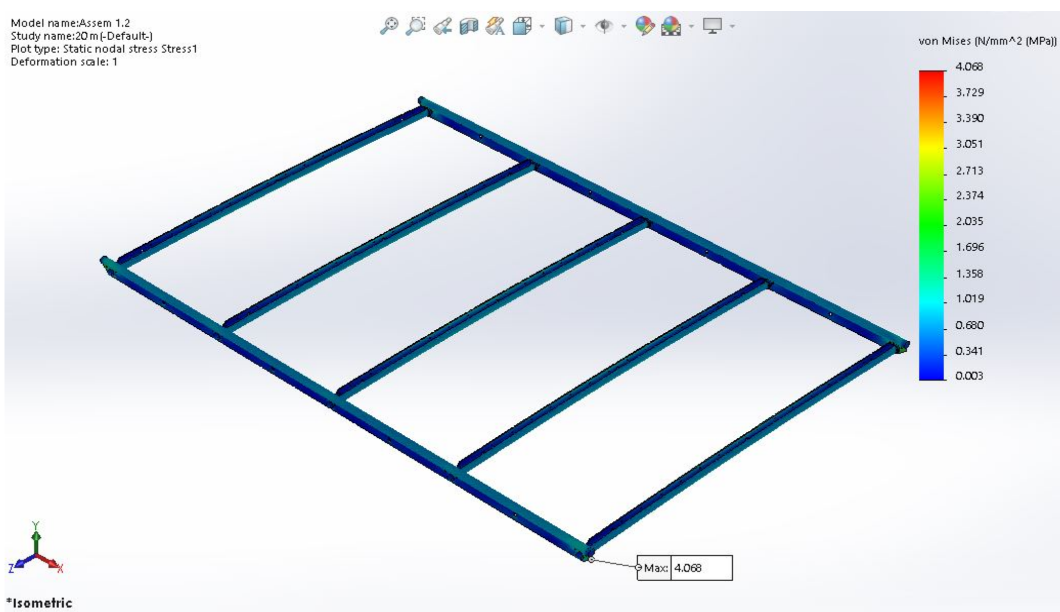

Fig. 4.45 Stress induced at 20 m depth

Displacement at 20 m depth on the module is represented below. Maximum displacement is 44.680 mm (see Fig. 4.46).

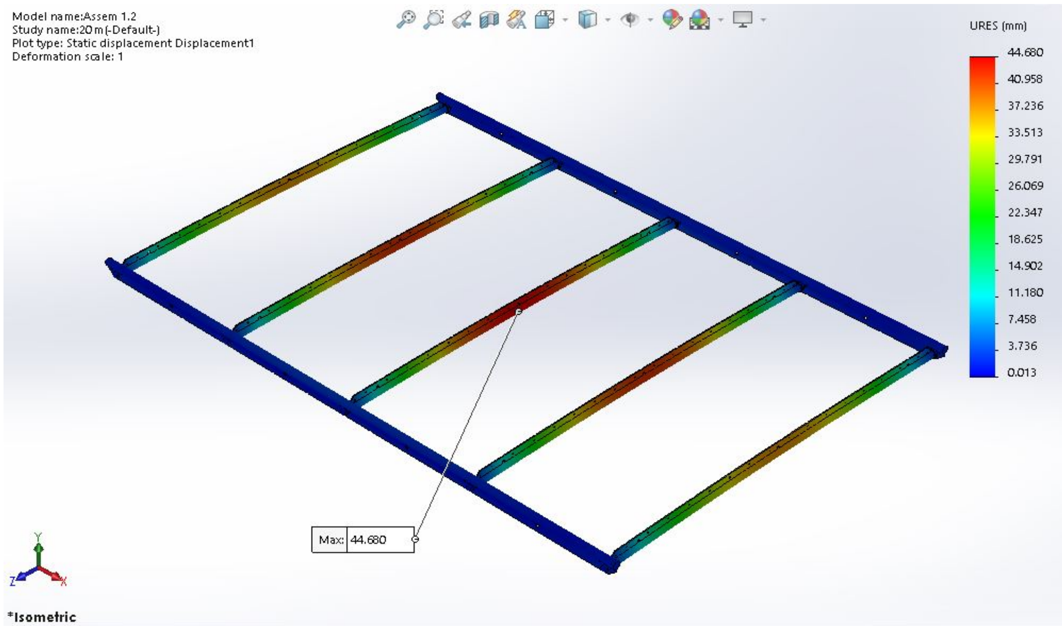

Fig. 4.46 Displacement at 20 m depth

f) 30 metre depth

Stress induced at 30 m depth on the module is represented below. Maximum stress induced is 4.967 MPa (see Fig. 4.47).

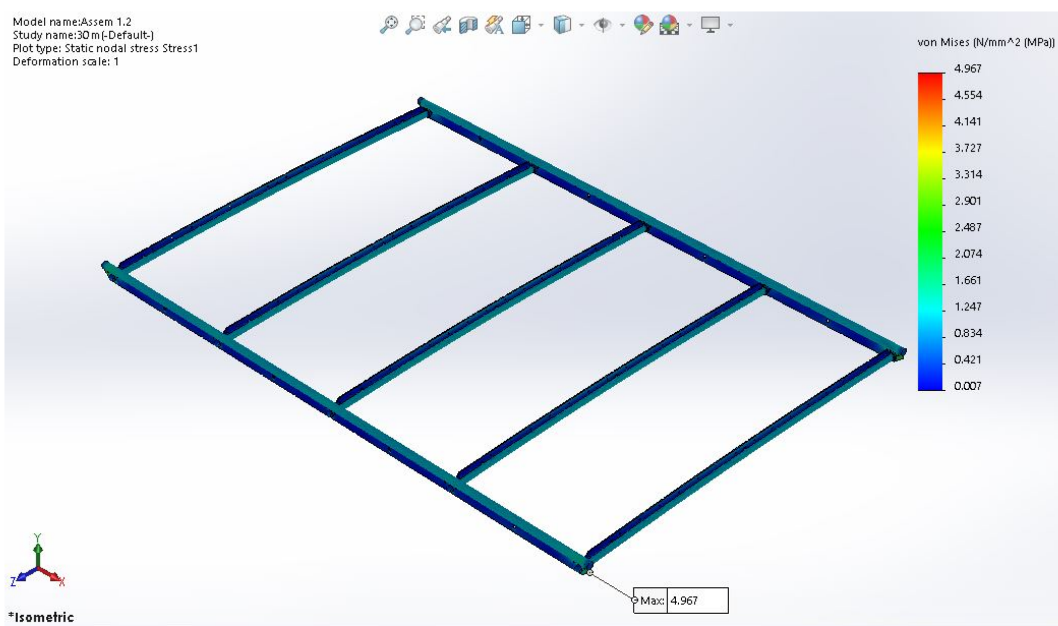

Fig. 4.47 Stress induced at 30 m depth

Displacement at 30 m depth on the module is represented below. Maximum displacement is 46.403 mm (see Fig. 4.48).

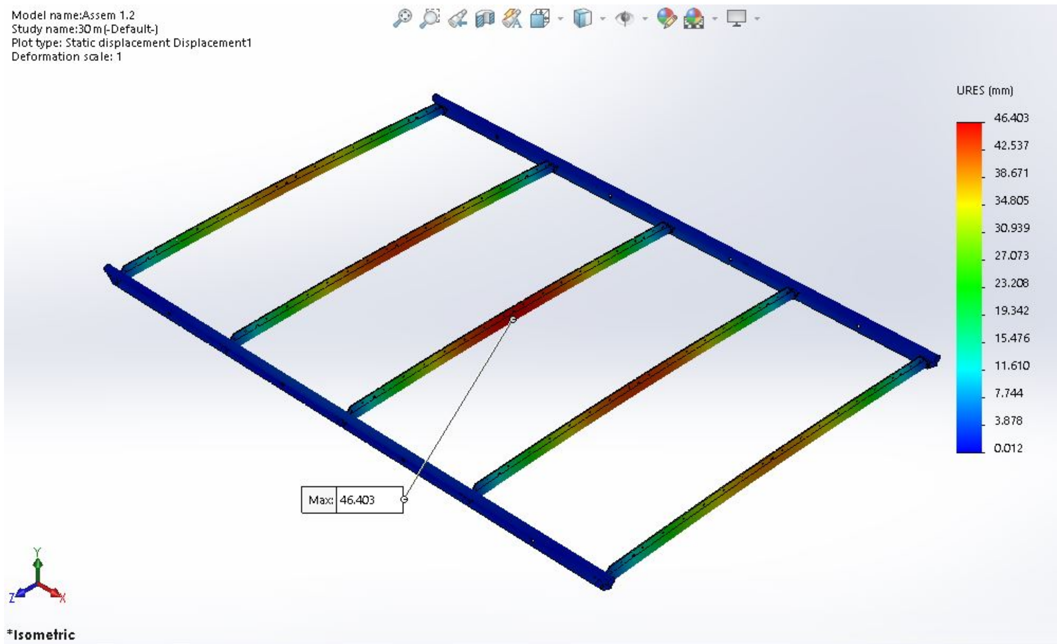

Fig. 4.48 Displacement at 30 m depth

4.3. Influence of flow

Let us see how flow of water acts on the module. The forces acting and change in stress due to these forces. For analyzing the effect of flow and calculating forces due to flow we used Solidworks Flow Simulation.

Following are the parameters considered for flow simulation;

a) Analysis type considered is external (see Fig. 4.49).

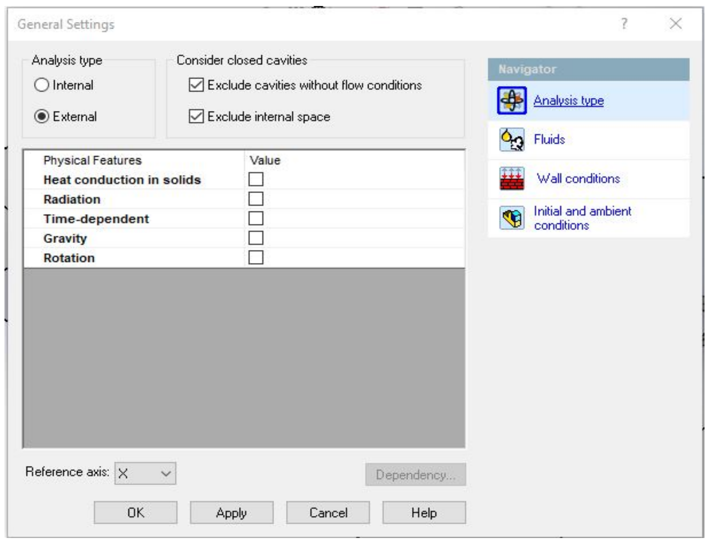

Fig. 4.49 Analysis type external

b) Fluid considered for analysis is water (see Fig. 4.50).

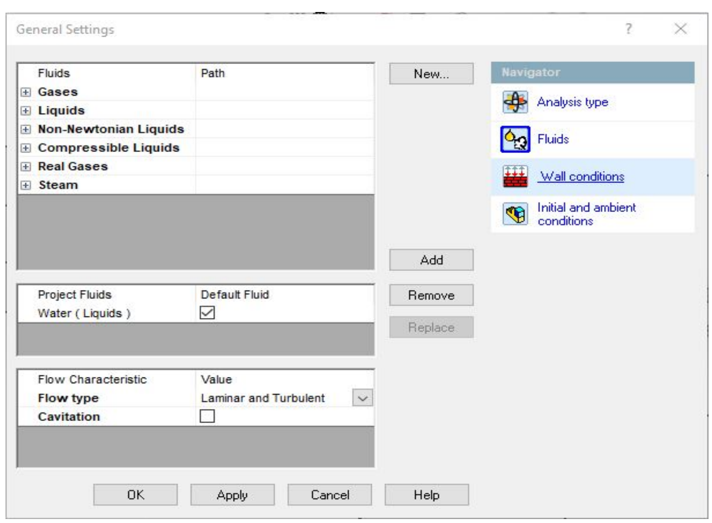

Fig. 4.50 Fluid considered for analysis

c) Wall conditions considered (see Fig. 4.51).

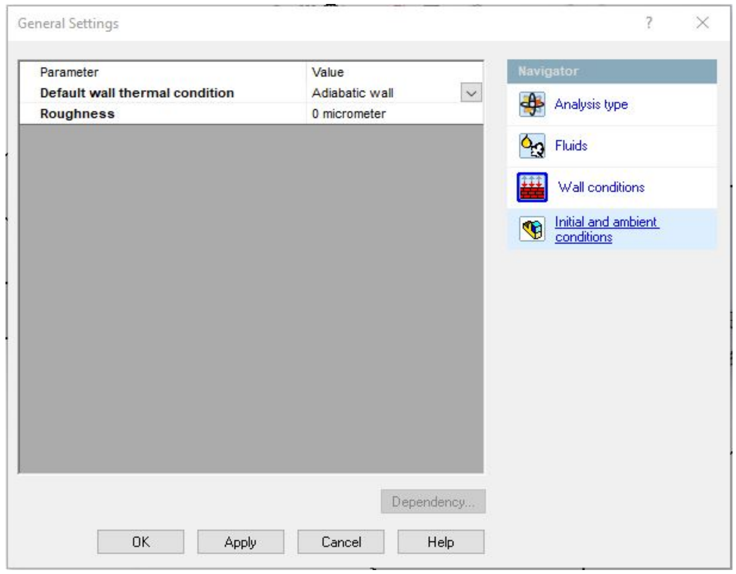

Fig. 4.51 Wall conditions

e) Initial and ambient conditions considered and velocity along X- direction is 1028.89 mm/s (see Fig. 4.52).

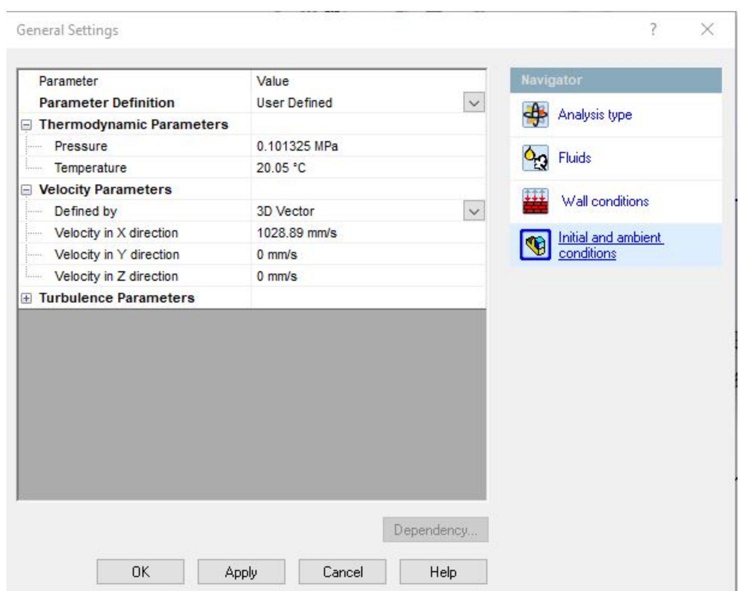

Fig. 4.52 Initial and ambient conditions applied

Forces acting along X- direction on different parts is shown in below Fig. 4.53 and their values are shown in table 4.1

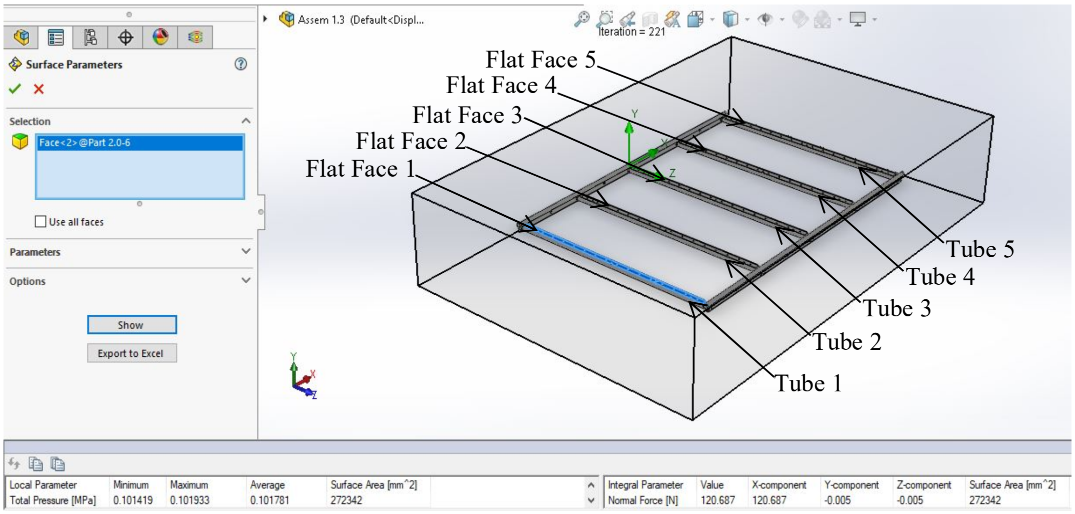

Fig. 4.53 Selections of faces to determine forces due velocity along X- direction

Table 4.1 Forces acting on different parts

Tube 1							
Flat Face							
Local Parameter	Maximum	Integral Parameter	Value	X- component	Y- component	Z- component	Surface Area [mm^2]
Total Pressure [MPa]	0.101933	Normal Force [N]	120.687	120.687	-0.005	-0.005	272342
Tube							
Local Parameter	Maximum	Integral Parameter	Value	X- component	Y- component	Z- component	Surface Area [mm^2]
Total Pressure [MPa]	0.102478	Normal Force [N]	206.788	165.954	-123.371	1.19E-04	875764

Tube 2							
Flat Face							
Local Parameter	Maximum	Integral Parameter	Value	X-component	Y-component	Z-component	Surface Area [mm^2]
Total Pressure [MPa]	0.101604	Normal Force [N]	17.683	17.683	-0.002	-0.002	272390
Tube							
Local Parameter	Maximum	Integral Parameter	Value	X-component	Y-component	Z-component	Surface Area [mm^2]
Total Pressure [MPa]	0.101706	Normal Force [N]	58.102	53.069	-23.653	-1.40E-02	877834
Tube 3							
Flat Face							
Local Parameter	Maximum	Integral Parameter	Value	X-component	Y-component	Z-component	Surface Area [mm^2]
Total Pressure [MPa]	0.101637	Normal Force [N]	38.907	38.907	-0.011	-0.011	272447
Tube							
Local Parameter	Maximum	Integral Parameter	Value	X-component	Y-component	Z-component	Surface Area [mm^2]
Total Pressure [MPa]	0.101684	Normal Force [N]	94.24	77.205	-54.042	-1.00E-03	881914
Tube 4							
Flat Face							
Local Parameter	Maximum	Integral Parameter	Value	X-component	Y-component	Z-component	Surface Area [mm^2]
Total Pressure [MPa]	0.101568	Normal Force [N]	30.803	30.803	-0.012	-0.012	272491

Tube							
Local Parameter	Maximum	Integral Parameter	Value	X-component	Y-component	Z-component	Surface Area [mm^2]
Total Pressure [MPa]	0.101644	Normal Force [N]	80.015	70.345	-38.133	3.53E-04	877774

Tube 5							
Flat Face							
Local Parameter	Maximum	Integral Parameter	Value	X-component	Y-component	Z-component	Surface Area [mm^2]
Total Pressure [MPa]	0.101555	Normal Force [N]	28.766	28.766	-0.014	-0.015	272539
Tube							
Local Parameter	Maximum	Integral Parameter	Value	X-component	Y-component	Z-component	Surface Area [mm^2]
Total Pressure [MPa]	0.101653	Normal Force [N]	81.419	74.161	-33.602	-1.95E-04	874676

Stress induced at 1 m depth on the module is represented below. Maximum stress induced is 6.786 MPa (see Fig. 4.54).

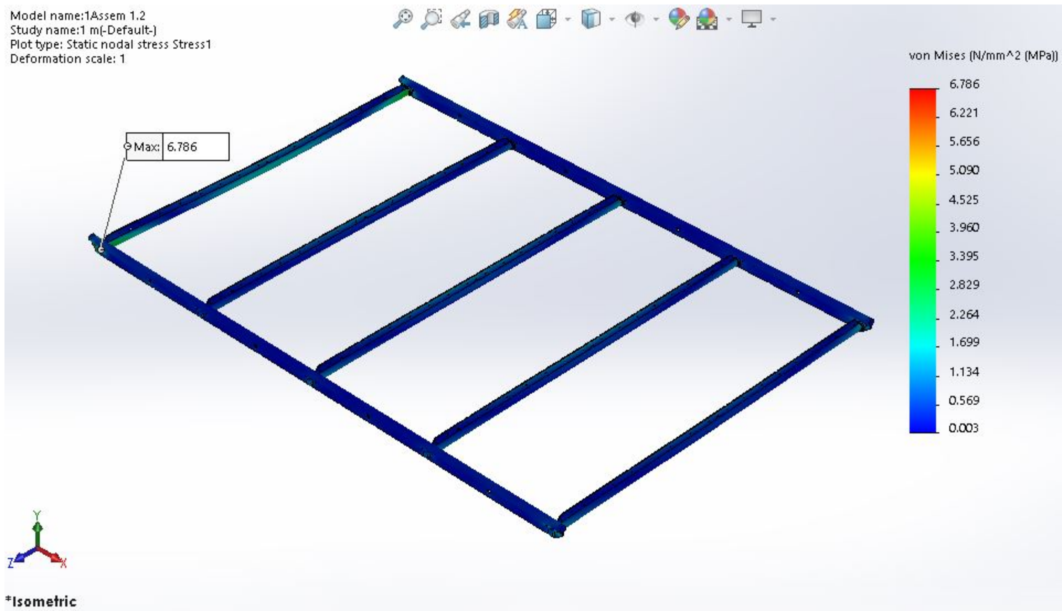

Fig. 4.54 Stress induced at 1 m depth

Displacement at 1 m depth on the module is represented below. Maximum displacement is 105.448 mm (see Fig. 4.55).

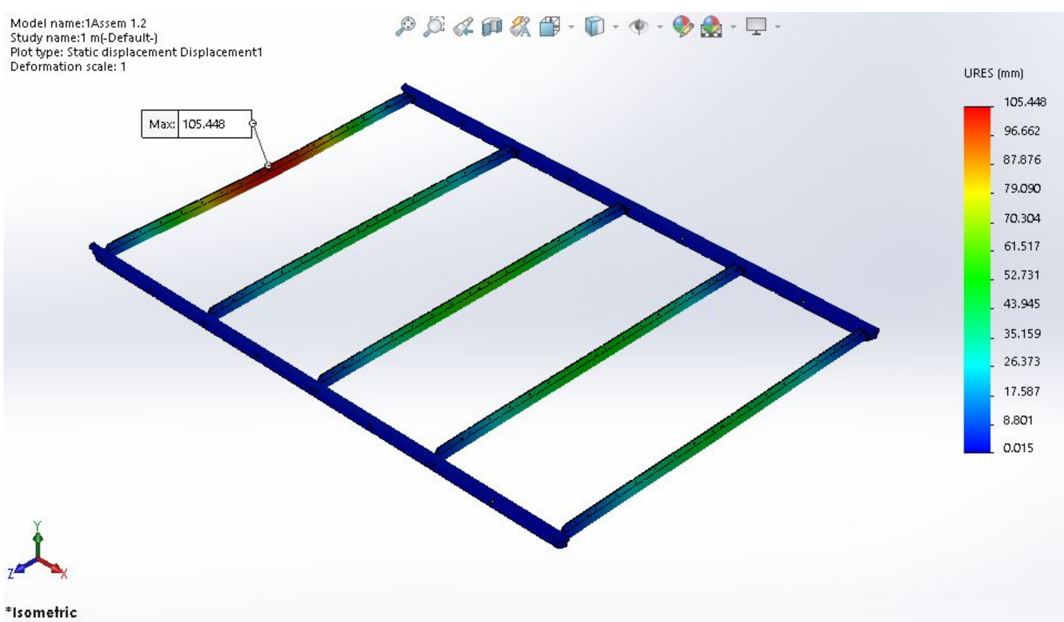

Fig. 4.55 Displacement at 1 m depth

Stress induced at 10 m depth on the module is represented below. Maximum stress induced is 6.790 MPa (see Fig. 4.56).

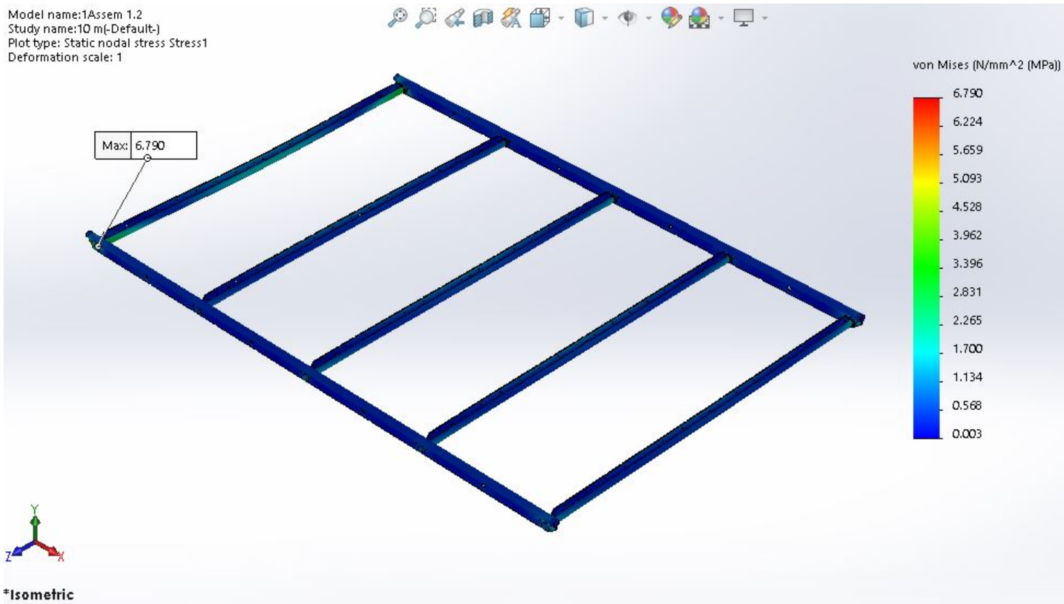

Fig. 4.56 Stress induced at 10 m depth

Displacement at 10 m depth on the module is represented below. Maximum displacement is 105.564 mm (see Fig. 4.57).

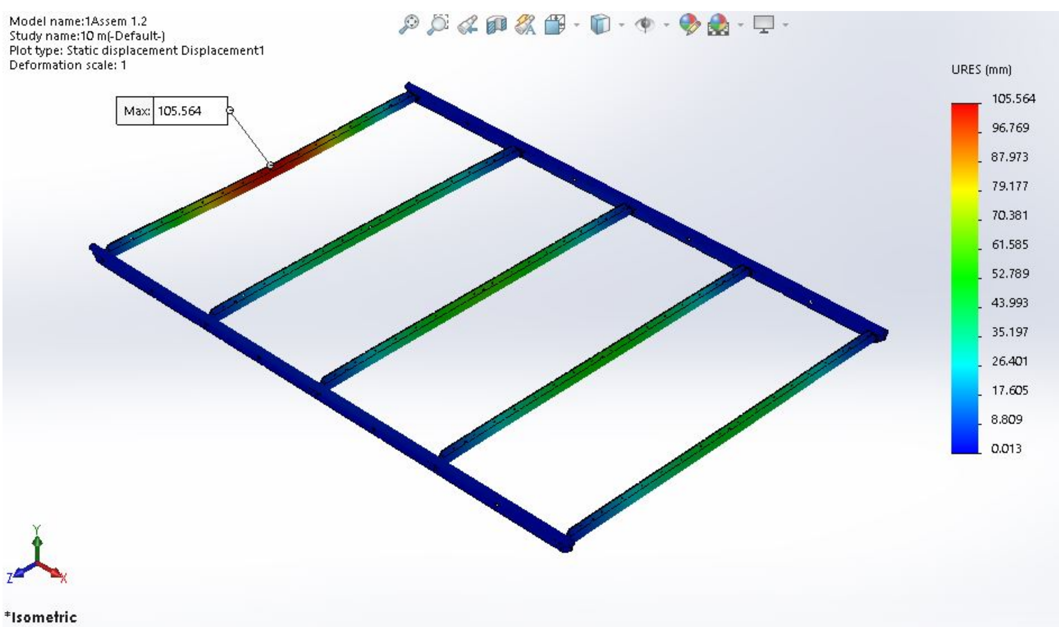

Fig. 4.57 Displacement at 10 m depth

Stress induced at 20 m depth on the module is represented below. Maximum stress induced is 6.930 MPa (see Fig. 4.58).

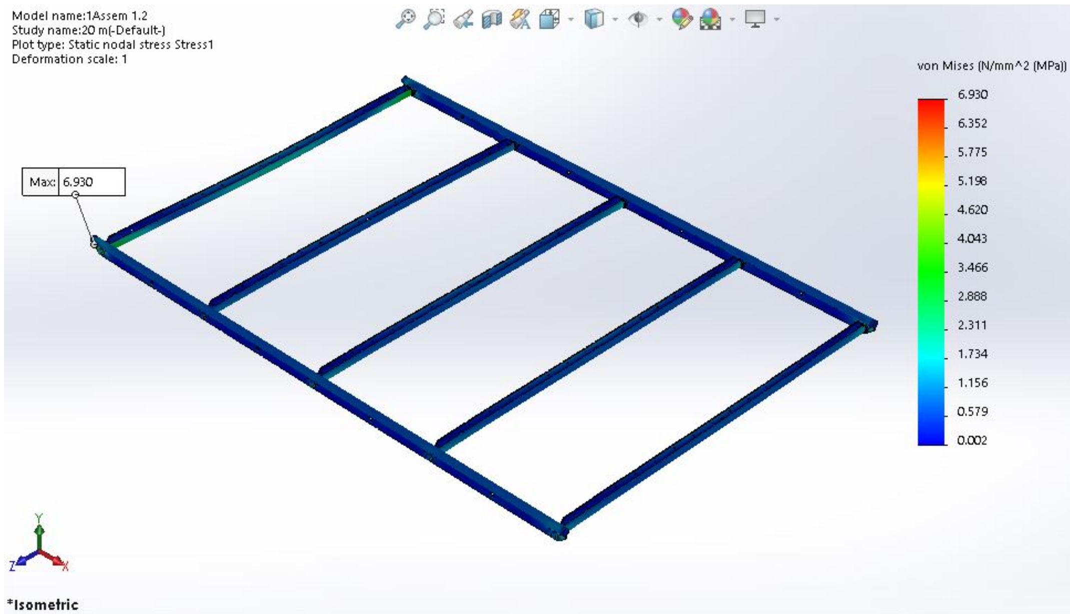

Fig. 4.58 Stress induced at 20 m depth

Displacement at 20 m depth on the module is represented below. Maximum displacement is 105.751 mm (see Fig. 4.59).

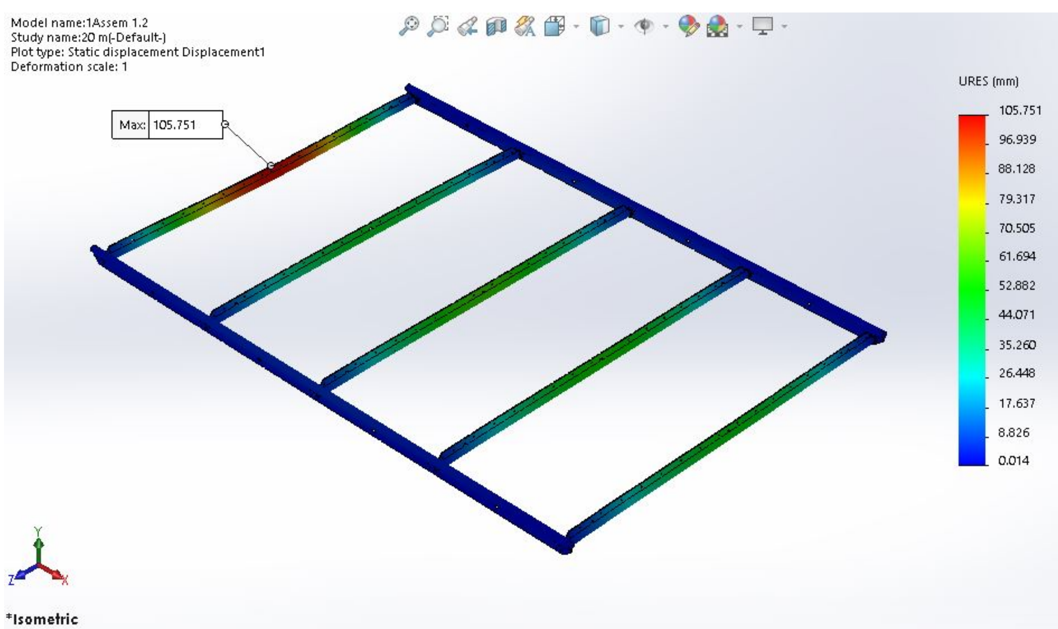

Fig. 4.59 Displacement at 20 m depth

Stress induced at 30 m depth on the module is represented below. Maximum stress induced is 7.907 MPa (see Fig. 4.60).

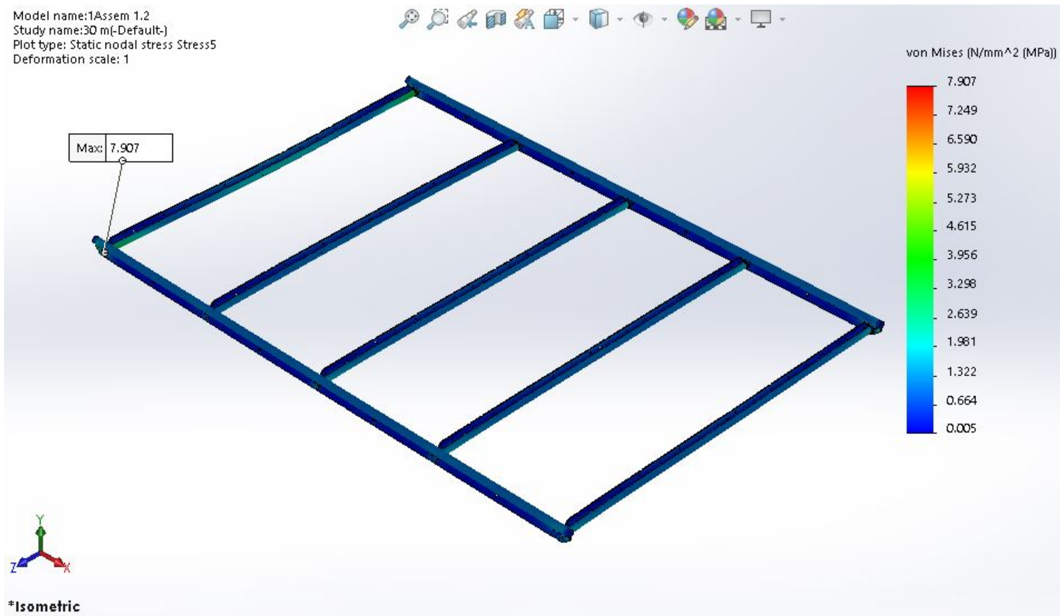

Fig. 4.60 Stress induced at 30 m depth

Displacement at 30 m depth on the module is represented below. Maximum displacement is 106.946 mm (see Fig. 4.61).

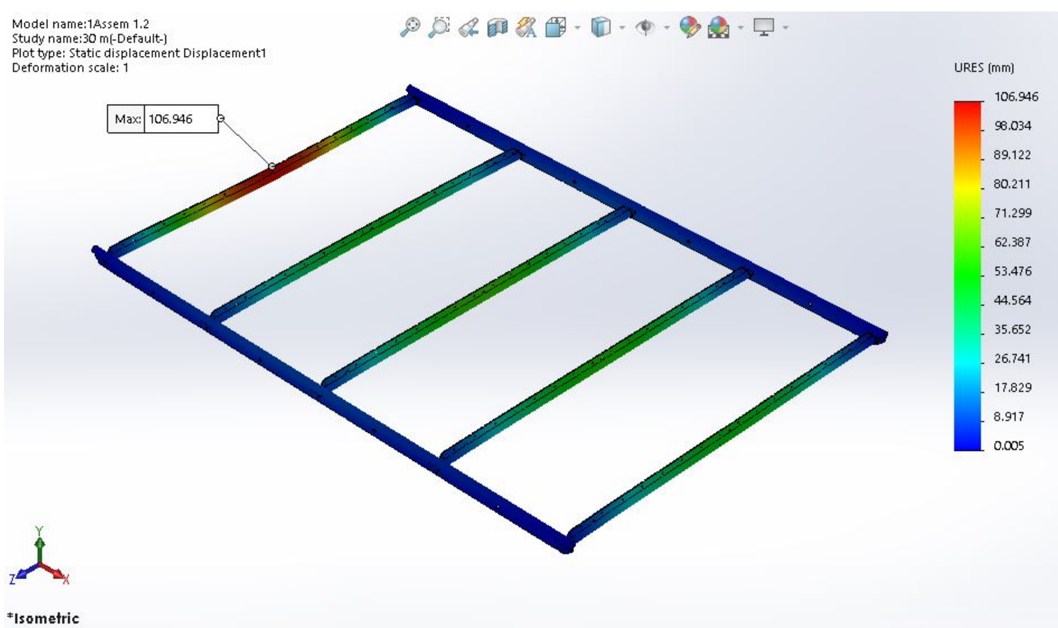

Fig. 4.61 Displacement at 30 m depth

5. RESULTS

Comparison between results for different depths

5.1. Maximum Stress

Table 5.1 Comparison of Stress

	Half Structure Maximum Stress, (MPa)	Whole Structure Maximum Stress, (MPa)
Gravitational Force	2.83	2.87
0 metre depth	3.81	3.95
1 metre depth	3.78	3.93
10 metre depth	3.48	3.77
20 metre depth	3.16	4.07
30 metre depth	2.95	4.97

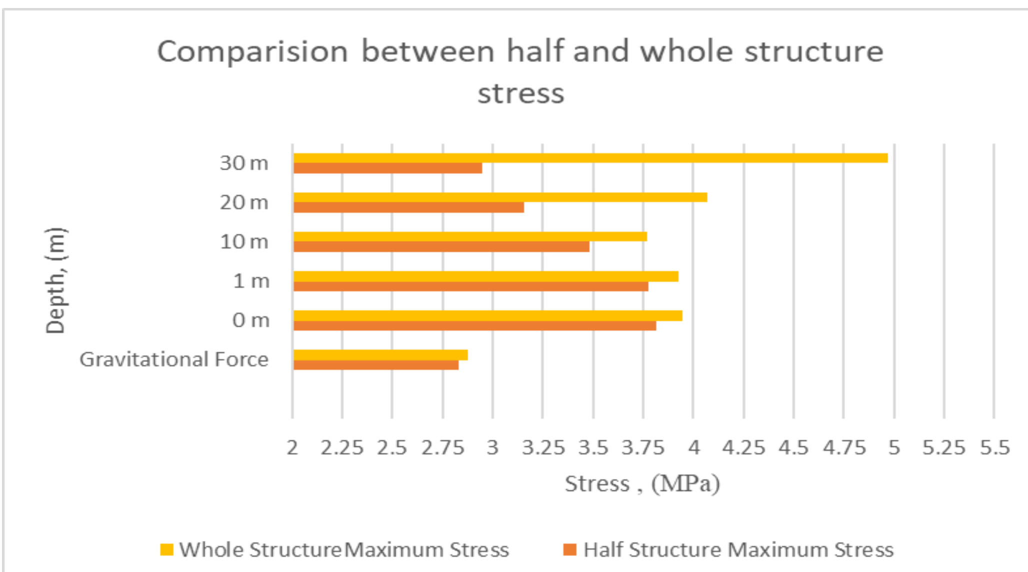

Fig. 5.1 Graphical representation of comparison of stress between half and whole structure

From above table 5.1 it can be seen that comparison of stress between half structure and whole structure is made. The stress caused are well within the range of tensile yield strength.

5.2. Maximum displacement

Table 5.2 Comparison of Displacement

	Half Structure Maximum Displacement, (mm)	Whole Structure Maximum Displacement, (mm)
Gravitational Force	33.13	27.80
0 metre depth	48.22	41.30
1 metre depth	48.65	41.47
10 metre depth	54.11	42.98
20 metre depth	62.65	44.68
30 metre depth	73.21	46.40

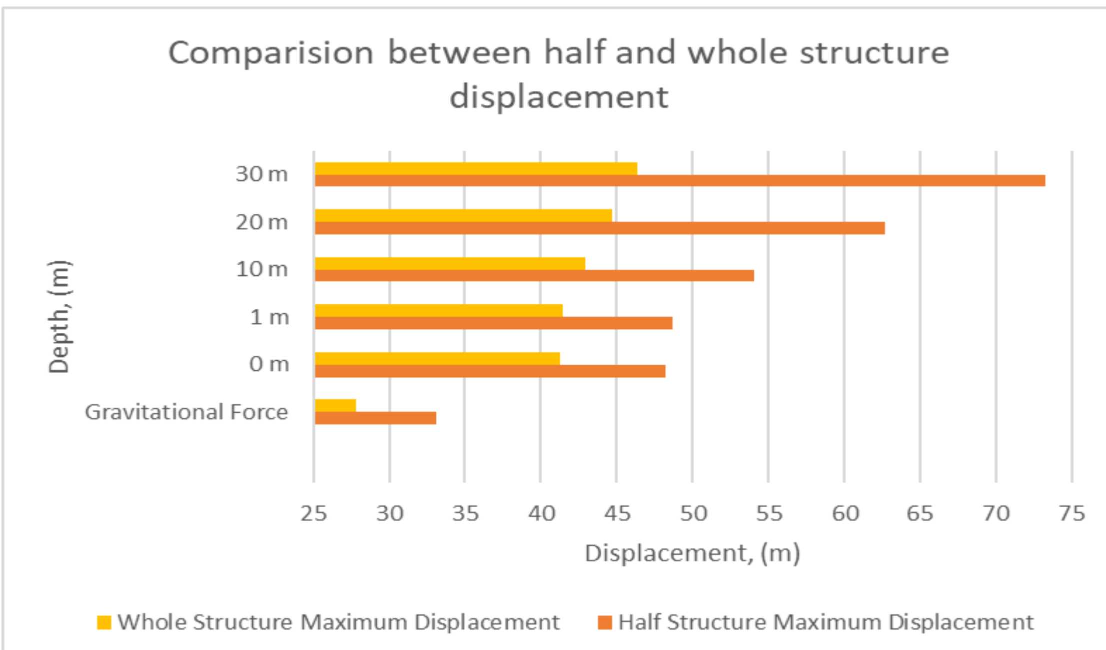

Fig. 5.2 Graphical representation of comparison of displacement between half and whole structure

From above table 5.2 it can be seen that comparison of displacement between half structure and whole structure is made. Displacement increases with increase in depth. The increase in displacement with increase in depth is due to rise in pressure

Comparison of results for different depths in consideration of velocity of water as 1028.89 mm/s.

5.3. Stress induced due to flow of water

Table 5.3 Comparison of Stress in consideration of influence of flow

	Half Structure Maximum Stress, without flow influence, (MPa)	Whole Structure Maximum Stress, without flow influence, (MPa)	Whole Structure Maximum Stress, with flow velocity at 1028.89 mm/s, (MPa)	Percentage change caused due to influence of flow, (%)
Gravitational Force	2.83	2.87	-	-
0 m	3.81	3.95	-	-
1 m	3.78	3.93	6.79	57.86%
10 m	3.48	3.77	6.79	55.52%
20 m	3.16	4.07	6.93	58.70%
30 m	2.95	4.97	7.91	62.82%

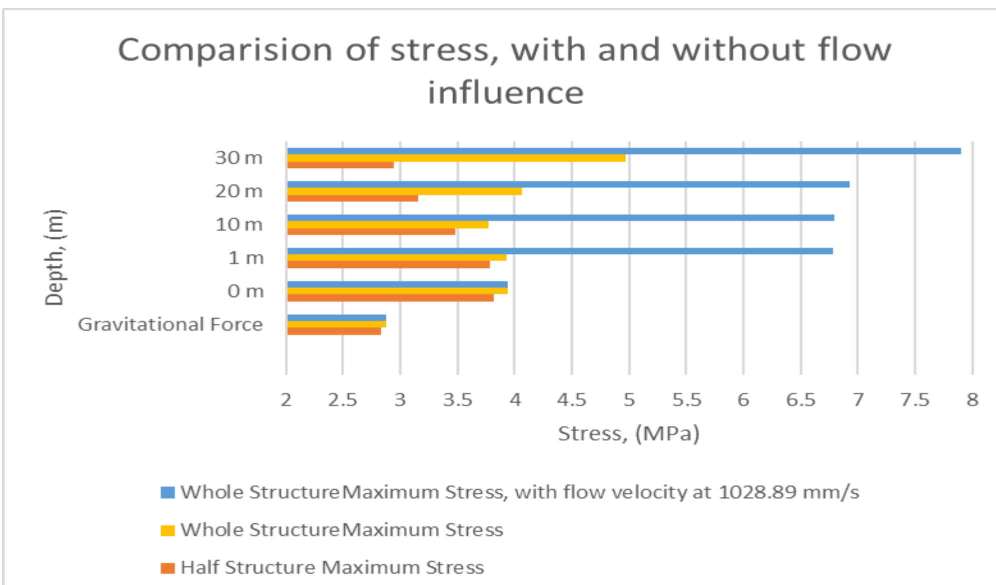

Fig. 5.3 Graphical representation of comparison of stress caused due to influence of flow

From above table it can be seen that how flow of water with velocity of 1028.89 mm/s influences on whole structure and effects the stresses at different depths when compared to without flow influence on whole structure.

5.4. Displacement due to flow of water

Table 5.4 Comparison of Displacement in consideration of influence of flow

	Half Structure Maximum Displacement, without flow influence, (mm)	Whole Structure Maximum Displacement, without flow influence, (mm)	Whole Structure Maximum Displacement, with flow velocity at 1028.89 mm/s, (mm)	Percentage change caused due to influence of flow, (%)
Gravitational Force	33.13	27.80	-	-
0 m	48.22	41.30	-	-
1 m	48.65	41.47	105.45	39.33%
10 m	54.11	42.98	105.56	40.71%
20 m	62.65	44.68	105.75	42.25%
30 m	73.21	46.40	106.95	43.39%

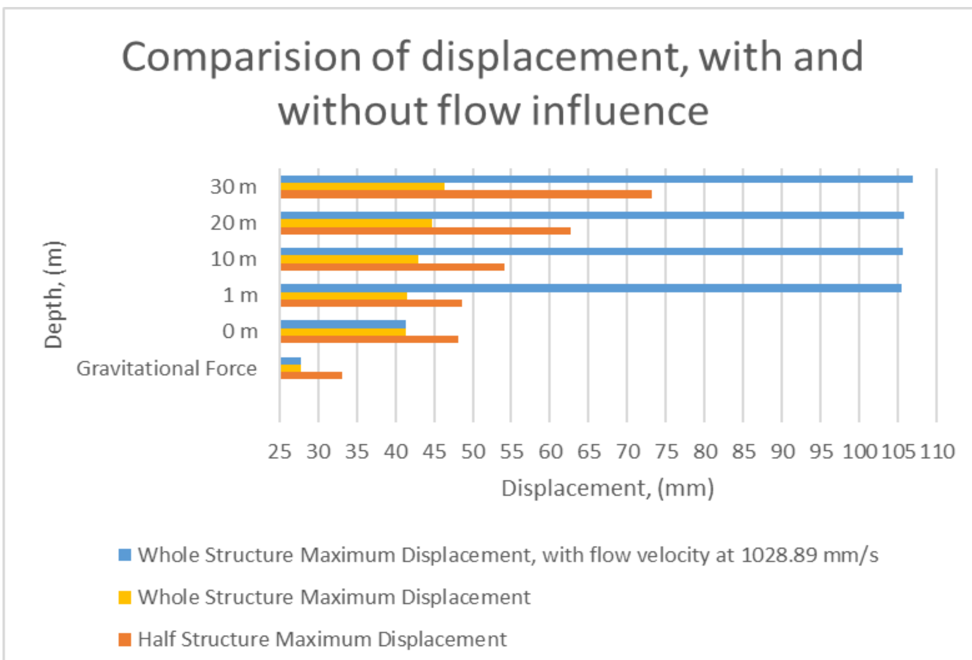

Fig. 5.1 Graphical representation of comparison of displacement caused due to influence of flow

From above table 5.4 it can be seen that how flow of water with velocity of 1028.89 mm/s influences on whole structure and effects the displacement at different depths when compared to without flow influence on whole structure. The increase in displacement with increase in depth is due to rise in pressure.

6. CONCLUSION

1. It can be concluded from analysis carried out that selected material for module can sustain without any failure. Min factor of safety of structure at 30 m depth without flow is about 400% and with flow is about 250%.
2. High stresses occurred places are not at critical points. They are at corner edges and holes which can be reduced by applying fillets. The stresses for whole structure is low and within the limits.
3. After obtaining and comparing the results of influence of flow with velocity to without influence of flow, it is seen that there is a 57.86- 62.82 % rise in stress and 39.33- 43.39 % rise in displacement at different depth.

REFERENCES

1. https://www.fisheries.noaa.gov/feature-story/milford-lab-takes-sugar-kelp-cultivation
2. https://www.scribd.com/document/135706004/Crompton-Physical-Testing-of-Plastics Pg. No. 1-2.
3. Jingyu Zhang. Experimental Study of Stress Cracking in High Density Polyethylene Pipes. *Drexel University doctoral thesis work, November 2005.* Pg. No. 1- 2
4. https://www.agru.at/fileadmin/user_upload/Prospekte/INDUSTRIEROHRSYSTEME/KAT-Industrial-piping-systems-technical-2017_WEBSC.pdf Pg. No. 108
5. https://www.agru.at/fileadmin/user_upload/Prospekte/INDUSTRIEROHRSYSTEME/KAT-Industrial-piping-systems-technical-2017_WEBSC.pdf Pg. No. 112
6. http://www.evopipes.lt/uploads/files/EvoSCGR_katalogs_2017_EN.pdf Pg. No. 13.
7. https://www.kau.edu.sa/Files/0057863/Subjects/Chapter%203.pdf Pg. No. 4-5